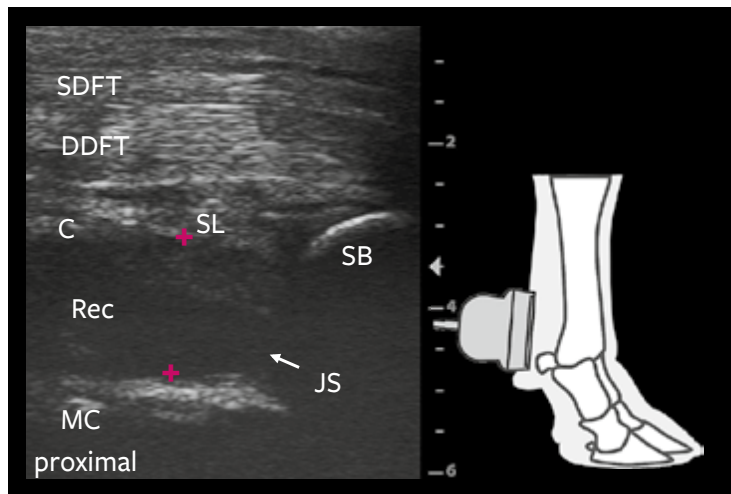


Johann Kofler (ed.)

Ultrasonography of the Bovine Musculoskeletal System

Indications, Examination protocols, Findings



Johann Kofler (ed.)

Ultrasonography of the Bovine Musculoskeletal System

*“Dedicated to my mentors
and all my enthusiastic teachers”*

Johann Kofler (ed.)

Ultrasonography of the Bovine Musculoskeletal System

Indications, Examination protocols, Findings

In collaboration with

Birgit Altenbrunner-Martinek

Kurt Bach

Javier Blanco Murcia

Naida Cristina Borges

Sébastien Buczinski

Sonja Franz

Arcangelo Gentile

Maike Heppelmann

Isabelle Masseur

Karl Nuss

Harald Pothmann

Michela Tatiana Re

Alexander Starke

Adrian Steiner

454 Figures and 5 Tables

schlütersche

Bibliographic information published by the German National Library [Deutsche Nationalbibliothek]

The German National Library has listed this publication in the German National Bibliography [Deutsche Nationalbibliografie].
Detailed bibliographic information is available on <https://dnb.de/>.

ISBN 978-3-89993-976-7 (print)

ISBN 978-3-8426-8961-9 (PDF)

Editor

Associate Prof., Dr. med. vet., Dip. ECBHM Johann Kofler
Department of Farm Animals and Veterinary Public Health
University Clinic for Ruminants, University of Veterinary Medicine Vienna
Veterinärplatz 1
1210 Vienna, Austria
johann.kofler@vetmeduni.ac.at

© 2021 Schlütersche Verlagsgesellschaft mbH & Co. KG, Hans-Böckler-Allee 7, 30173 Hannover, Germany

This work is protected by copyright. All rights reserved by the publisher.

In the absence of the publisher's written consent, any exploitation outside of the cases provided for by law is impermissible and a punishable offence. This also applies to any reproduction of parts of the book. Product and company names may be protected under trademark law without being specially identified in the book. The described characteristics and modes of action of the aforementioned pharmacological preparations are based on the experiences of the authors, who have taken the utmost care to ensure that all therapeutic details provided correspond to the state of knowledge and research prevailing at the time when the book goes to print. Notwithstanding this, the information enclosed with the products, as well as the manufacturers' specialised information must, in any event, be observed during the selection, use and dosing of therapies, medication and other products; in cases of doubt, a suitable specialist is to be consulted. Neither the publisher nor the authors accept any liability for product characteristics, delivery obstacles or incorrect use or in the event of any accidents or cases of damage, loss or injury occurring. Every user is obliged to carefully check the medication to be carried out. The user is responsible for every medication, dosage or application.

Project management: Sabine Poppe, Hannover, Germany

Copy editing: Dr. med. vet. Nicole Wackwitz, Adelheidsdorf, Germany

Cover design and image editing: Jessica Mora-Lara, Hannover, Germany

Typesetting and Layout: Sandra Knauer Satz·Layout·Service, Garbsen, Germany

Printing Company: xxxxxxxx, Germany

Contents

Authors	IX	2.4	General ultrasonographic findings in arthritis, tenosynovitis, bursitis, abscesses and hematomas	12
Preface	XI			
1	Principles of ultrasonographic imaging of the bovine musculoskeletal system ..	1		
	<i>Sébastien Buczinski, Isabelle Masseur</i>			
1.1	Introduction	1		
1.2	Physics and acoustic principles	1		
1.2.1	Specular reflection	2	2.4.1	Arthritis, tenosynovitis and bursitis
1.2.2	Diffuse reflection (scattering)	3	2.4.2	Abscesses and hematomas
1.2.3	Attenuation	3	2.5	Conclusions
1.2.4	Axial, lateral and elevational resolution	3		24
1.3	Artifacts	4	3	Ultrasonographic examination of the distal and proximal interphalangeal joint regions
1.3.1	Artifacts associated with resolution problems	5		25
1.3.2	Refraction or double image artifacts	5		<i>Maïke Heppelmann, Alexander Starke, Johann Kofler</i>
1.3.3	Reverberation artifact	5	3.1	Introduction
1.3.4	Comet-tail and ring-down artifacts	5	3.2	Indications for ultrasonographic examination
1.3.5	Distal acoustic enhancement	6	3.3	Anatomy
1.3.6	Distal acoustic shadowing artifact	7	3.4	Ultrasonographic examination procedure and anatomical landmarks
1.3.7	Edge shadowing artifact	8	3.5	Normal ultrasonographic appearance of the anatomical structures
1.3.8	Fan or other electrical induced artifacts	8	3.6	Sonopathological findings
1.4	Probes and frequencies	9	3.6.1	Arthritis of the DIJ
1.5	Preparation of the patient and the region of interest	9	3.6.2	Arthritis of the PIJ
1.6	Orientation and use of a standardized ultrasonographic examination protocol ..	9	3.6.3	Osteitis and osteomyelitis
1.7	Description of findings and documentation	10		
2	Ultrasonography of arthritis, tenosynovitis, bursitis, abscesses, hematomas – general findings	11	4	Ultrasonographic examination of the metacarpo- and metatarsophalangeal joint regions
	<i>Johann Kofler, Adrian Steiner, Alexander Starke, Karl Nuss</i>			35
2.1	Introduction	11		<i>Johann Kofler</i>
2.2	Ultrasonographic examination technique for exudate-filled cavities	11	4.1	Introduction
2.3	Normal ultrasonographic appearance of joints, tendon sheaths and bursae	12	4.2	Indications for ultrasonographic examination
			4.3	Anatomy
			4.4	Ultrasonographic examination procedure and anatomical landmarks
			4.5	Normal ultrasonographic appearance of the anatomical structures
			4.6	Sonopathological findings
			4.6.1	Arthritis
			4.6.2	Osteitis and osteomyelitis

4.6.3	Edema, abscesses and thromboses	47		
4.6.4	Collateral ligament tears, luxation/ subluxation and adjoining physal fracture ..	48		
5	Ultrasonographic examination of the carpal region	51		
	<i>Johann Kofler, Karl Nuss</i>			
5.1	Introduction	51		
5.2	Indications for ultrasonographic examination	51		
5.3	Anatomy	52		
5.4	Ultrasonographic examination procedure and anatomical landmarks	52		
5.5	Normal ultrasonographic appearance of the anatomical structures	54		
5.6	Sonopathological findings	55		
5.6.1	Carpal arthritis	55		
5.6.2	Osteitis and osteomyelitis	61		
5.6.3	Precarpal bursitis (precarpal hygroma)	62		
5.6.4	Tenosynovitis of the carpal extensor and flexor tendon sheaths	63		
5.6.5	Edema and abscesses	64		
6	Ultrasonographic examination of the elbow region	67		
	<i>Naida Cristina Borges, Johann Kofler</i>			
6.1	Introduction	67		
6.2	Indications for ultrasonographic examination	67		
6.3	Anatomy	67		
6.4	Ultrasonographic examination procedure and anatomical landmarks	68		
6.5	Normal ultrasonographic appearance of the anatomical structures	70		
6.6	Sonopathological findings	72		
6.6.1	Arthritis	72		
6.6.2	Osteitis and osteomyelitis	75		
6.6.3	Fractures, subluxations and osteoarthritis ..	75		
7	Ultrasonographic examination of the shoulder region	79		
	<i>Birgit Altenbrunner-Martinek, Karl Nuss, Alexander Starke, Johann Kofler</i>			
7.1	Introduction	79		
7.2	Indications for ultrasonographic examination	79		
7.3	Anatomy	79		
7.4	Ultrasonographic examination procedure and anatomical landmarks	81		
7.5	Normal ultrasonographic appearance of the anatomical structures	82		
7.5.1	Scapula and humerus	82		
7.5.2	Scapulohumeral joint, bicipital and infraspinous bursa	82		
7.5.3	Tendons and muscles	82		
7.6	Sonopathological findings	84		
7.6.1	Arthritis	84		
7.6.2	Bursitis	86		
7.6.3	Osteomyelitis, osteitis, avulsion fractures and luxation	87		
7.6.4	Periarticular abscess	88		
8	Ultrasonographic examination of the tarsal region	89		
	<i>Karl Nuss, Johann Kofler</i>			
8.1	Introduction	89		
8.2	Indications for ultrasonographic examination	89		
8.3	Anatomy	90		
8.4	Ultrasonographic examination procedure and anatomical landmarks	93		
8.5	Normal ultrasonographic appearance of anatomical structures	94		
8.6	Sonopathological findings	96		
8.6.1	Tarsal arthritis	96		
8.6.2	Lateral tarsal hygroma/bursitis	100		
8.6.3	Disorders of the calcaneal tuber region	100		
9	Ultrasonographic examination of the stifle region	105		
	<i>Johann Kofler, Alexander Starke, Karl Nuss</i>			
9.1	Introduction	105		
9.2	Indications for ultrasonographic examination	105		
9.3	Anatomy	106		
9.4	Ultrasonographic examination procedure and anatomical landmarks	107		
9.5	Normal ultrasonographic appearance of the anatomical structures	109		
9.6	Sonopathological findings	112		
9.6.1	Stifle arthritis	112		
9.6.2	Osteitis, osteomyelitis and osteochondrosis	116		
9.6.3	Stifle ligament and meniscal injuries	118		
9.6.4	Stifle bursitis	119		
9.6.5	Abscesses and seromas	120		

10	Ultrasonographic examination of the coxofemoral joint and pelvic region	121	13	Ultrasonographic examination of limb vessels	159
	<i>Johann Kofler, Alexander Starke, Karl Nuss</i>			<i>Johann Kofler, Alexander Starke</i>	
10.1	Introduction	121	13.1	Introduction	159
10.2	Indications for ultrasonographic examination	121	13.2	Indication for the ultrasonographic examination	160
10.3	Anatomy	122	13.3	Anatomy	160
10.4	Ultrasonographic examination procedure and anatomical landmarks	124	13.4	Ultrasonographic examination procedure	163
10.5	Normal ultrasonographic appearances of the anatomical structures	125	13.5	Normal ultrasonographic appearance of arteries and veins	164
10.6	Sonopathological findings	128	13.6	Sonopathological findings	168
10.6.1	Coxofemoral arthritis	128	13.6.1	Thrombosis	168
10.6.2	Coxofemoral luxation	131	13.6.2	Calcinosis	172
10.6.3	Fractures	132	13.6.3	Varicosity	174
10.6.4	Degenerative joint disease	134	13.6.4	Pathological PW-Color Doppler flow characteristics	174
10.6.5	Muscle lesions, abscesses, hematomas, nerve injuries, thromboses and tumors	135			
11	Ultrasonographic examination of flexor and extensor tendons, tendon sheaths and the suspensory ligament	137	14	Ultrasonographic imaging of bone lesions	175
	<i>Karl Nuss, Johann Kofler</i>			<i>Johann Kofler, Adrian Steiner, Alexander Starke, Karl Nuss</i>	
11.1	Introduction	137	14.1	Introduction	175
11.2	Indication for ultrasonographic examination	137	14.2	Indication for ultrasonographic examination of the bone	175
11.3	Anatomy	138	14.3	Anatomy of bone	175
11.4	Ultrasonographic examination procedure and anatomical landmarks	138	14.4	Normal ultrasonographic appearance of bone surfaces	176
11.5	Normal ultrasonographic appearance of the anatomical structures	140	14.5	Ultrasonographic findings on bone surfaces	177
11.6	Sonopathological findings	142	14.5.1	Fractures and fissures	177
11.6.1	Tear or rupture of tendons/ligaments	142	14.5.2	Subluxation and luxation	182
11.6.2	Septic inflammation of tendon sheaths and tendons	144	14.5.3	Osteitis and osteomyelitis	183
			14.5.4	Bone sequestrum	187
			14.5.5	Osteochondrosis and osteoarthritis	189
			14.5.6	Bone-associated tumors	192
12	Ultrasonographic examination of muscles	147	14.6	Conclusions	192
	<i>Karl Nuss, Johann Kofler</i>				
12.1	Introduction	147	15	Ultrasonographic imaging and measurement of sole horn and digital fat cushion thicknesses	193
12.2	Indication for ultrasonographic examination	148		<i>Kurt Bach, Johann Kofler</i>	
12.3	Anatomy	148	15.1	Introduction	193
12.4	Ultrasonographic examination procedure and anatomical landmarks	149	15.2	Indication for ultrasonographic examination	194
12.5	Normal ultrasonographic appearance of the anatomical structures	150	15.3	Anatomy	194
12.6	Sonopathological findings	152	15.4	Ultrasonographic examination procedure and anatomical landmarks	195
			15.5	Normal ultrasonographic appearance of the anatomical structures	196

15.6	Sonopathological findings	198	17.6	Normal ultrasonographic appearance ...	216
15.6.1	Thin soles	198	17.6.1	Normal ultrasonographic appearance of the brachial plexus	217
15.6.2	Changes in the digital cushion (sole's soft tissue) thickness	200	17.6.2	Normal ultrasonographic appearance of the sciatic nerve	217
15.6.3	Alterations of the surface of the distal phalanx	201	17.6.3	Normal ultrasonographic appearance of the femoral nerve	219
15.6.4	Fractures of the pedal bone	203	17.7	Sonopathological findings	219
16	Ultrasonographic measurement of backfat thickness	205	18	Ultrasonographic imaging of the spinal cord	221
	<i>Harald Pothmann</i>			<i>Sonja Franz, Arcangelo Gentile</i>	
16.1	Introduction	205	18.1	Introduction	221
16.2	Indications for ultrasonographic measurement of BFT	205	18.2	Indication for spinal ultrasonography ...	222
16.3	Anatomy	206	18.3	Anatomy	222
16.4	Ultrasonographic examination procedure and anatomical landmarks	206	18.4	Ultrasonographic examination procedure for the spinal cord and anatomical landmarks	223
16.5	Normal ultrasonographic appearance of the anatomical structures	207	18.5	Normal ultrasonographic appearance of the spinal cord in the three acoustic windows	226
16.6	Reference values for different breeds ...	208	18.5.1	Atlanto-occipital acoustic window	226
16.7	Correlation of BFT with BCS	208	18.5.2	Lumbar acoustic window	226
			18.5.3	Lumbo-sacral acoustic window	228
17	Ultrasonographic imaging of large nerves and ultrasound-guided nerve blocks of the limbs	211	18.6	Ultrasound-guided collection of cerebrospinal fluid	228
	<i>Michela Tatiana Re, Javier Blanco-Murcia</i>		18.7	Sonopathological findings of the spinal cord	229
17.1	Introduction	211	19	Ultrasound-guided joint and soft tissue interventions	233
17.2	Principles of ultrasound-guided nerve block	211		<i>Johann Kofler</i>	
17.2.1	Advantages of ultrasound guided nerve block	211	19.1	Introduction	233
17.2.2	Needle insertion technique	211	19.2	Indications for ultrasound-guided joint and soft tissue interventions	233
17.3	Indications for ultrasound-guided nerve blocks	213	19.3	Application procedure	234
17.3.1	Indications for forelimb anesthesia: brachial plexus block	213	Appendix	239	
17.3.2	Indication for hindlimb anesthesia: sciatic and femoral nerve block	213	References	240	
17.4	Anatomy of the brachial plexus and the sciatic and femoral nerves	213	Index	253	
17.4.1	Brachial plexus	213			
17.4.2	Sciatic nerve	213			
17.4.3	Femoral nerve	214			
17.5	Ultrasonographic examination procedure and anatomical landmarks	214			
17.5.1	Brachial plexus	214			
17.5.2	Sciatic nerve	214			
17.5.3	Femoral nerve	216			

Preface

Ultrasonographic examination of the bovine musculoskeletal system was described in the mid-nineties for the first time and has become today a routinely applied ancillary diagnostic imaging technique in many veterinary teaching hospitals worldwide.

The goal of this textbook is to demonstrate to all cattle veterinarians the large variety of indications for ultrasonographic examination in bovine patients with musculoskeletal disorders. In particular, we want to provide detailed guidance on how the region of interest can be scanned correctly, which type and frequency of probes are adequate, to present the normal ultrasonographic appearance and to illustrate the most common pathological conditions.

We are required to make decisions during each clinical/orthopedic examination. However, clinical/orthopedic findings alone are often not sufficient to reach a diagnosis in bovine orthopedic patients. The additional use of diagnostic ultrasound may enable the clinician to state a definitive diagnosis, and to make a well-founded decision regarding prognosis and treatment. This includes the targeted administration of antimicrobial agents.

“Ultrasonography is the continuation of the clinical examination with other tools”: This statement was made in 1976 by the medical internist G. Rettenmaier, and still today I believe it precisely describes the paramount value of diagnostic ultrasound for the clinician in daily practice. It can be applied independently of location and time. Similar to the clinical exam, which follows a given examination schedule, the accurate ultrasonographic examination adheres to a standardized protocol, where the sonographer scans all the structures located in the region of interest in a certain sequence, in order to not overlook lesions, masses, or incriminated structures, which may not be clinically apparent.

Furthermore, the ultrasound probe is employed by the sonographer much like the fingers of his/her own hand during a clinical exam: The sonographer uses the probe for so-called sonopalpation, to classify the content of synovial cavities or other swellings as liquid, semi-solid, or solid effusions, to differentiate limb arteries and veins, and to diagnose thrombus formation.

The advantage of uniting the clinician and sonographer is that this person is fully familiar with the anatomic site in question as well as the clinical findings. Diagnostic ultrasound is a safe and non-invasive procedure for the patient, the sonographer and nearby personnel. Moreover, it is well suited for serial examinations to monitor the progression of the condition and response to treatment.

This is the first textbook on bovine musculoskeletal ultrasound composed by international experts that covers all parts of the bovine musculoskeletal system that can be involved in patients presented with lameness. The chapters in this textbook focus on specific joint regions of the limbs (e.g. fetlock, carpal, tarsal and other joint regions). These correspond to common experience with bovine orthopedic patients, where mainly one limb region is affected, but also occasionally where there is more than one defined limb region involved (most frequently in calves).

Each chapter is structured in the same manner: After a brief introduction, important indications for the ultrasonographic examination of individual regions are listed, followed by a brief anatomical overview, the presentation of anatomical landmarks and standard ultrasonographic views for the region of interest. This is followed by a detailed description of the ultrasonographic examination method for the particular region, and the normal ultrasonographic appearance of the most important anatomical structures. Finally, the ultrasonographic findings of the most common pathological conditions of the particular region are presented. Many sonograms illustrating normal appearances and the ultrasonographic findings of the most frequent disorders complete each chapter.

Additionally, there is an introductory chapter explaining the most important principles of diagnostic ultrasound, and the most common artifacts encountered during ultrasonographic examination. This textbook also contains a chapter on ultrasonographic imaging and measurement of the thickness of sole horn and the sole's soft tissue layer, which is an important research topic today. This is completed by a chapter on the ultrasonographic measurement of the back fat thickness.

Besides the description of the ultrasonographic inspection of all (joint) regions of the limbs, additional chapters focus on the general ultrasonographic evaluation of synovial cavities, tendons and ligaments, muscles, vessels, large peripheral nerves and the spinal cord. These structures are important for the physiological function of the bovine musculoskeletal system. Maybe surprising for ultrasound newcomers, one chapter focuses on the ultrasonographic examination of bone surfaces and imaging of numerous associated bone alterations. The textbook is completed by a chapter on ultrasound-guided centesis of synovial cavities, ultrasound-guided fine-needle aspiration and biopsy collection.

I want to sincerely thank all the internationally recognized experts and authors for their contributions to this textbook, enabling a unique and comprehensive overview of all the indications and possible applications of diagnostic ultrasound in bovine orthopedic patients.

The authors of this textbook would like to encourage all cattle veterinarians in clinics and, in particular, in bovine

practice, to improve their ultrasonographic regional skills of the bovine musculoskeletal system. We want to inspire bovine practitioners to use their already available ultrasound units and probes already used for bovine reproduction to improve diagnosis of bovine musculoskeletal disorders.

My proposed slogan for enthusiastic colleagues all over the world engaged in cattle (and of course with other species) health management is: *Diagnostic ultrasound is the best friend of the clinician, it is available everywhere and at any time*, and it is well suited to support immediate decision making in clinics and on-farm settings.

When a thorough clinical/orthopedic examination does not lead to a final diagnosis, *always ask your best friend*. When you visit an orthopedic bovine patient, follow the slogan “*yes, we scan!*”!

Vienna, February 2021

Johann Kofler

Acknowledgements

I wish to thank Cameron R. McCulloch, PhD, University of Veterinary Medicine Vienna, for reading the text and providing language assistance.

I would like to acknowledge Mrs. Anna E. Vogl (Mödling, Austria); she designed all the illustrations that are attached to all sonograms demonstrating the exact placement of the probe to achieve the presented ultrasonographic image.

1 Principles of ultrasonographic imaging of the bovine musculoskeletal system

Sébastien Buczinski, Isabelle Masseur

1.1 Introduction

Ultrasonography is an imaging technique based on the reflection and refraction of acoustic waves as they are transmitted through the tissues (Kirberger 1995). In veterinary medicine, it was initially applied to the diagnosis of pregnancy, to assess reproductive organs prior to insemination or in an attempt to determine causes of failure to induce pregnancy in cattle. Its affordable cost and ease of use have contributed to its popularity and explain that today many veterinary practitioners are equipped with an ultrasound machine dedicated to cattle reproduction management programs (King 2006, DesCôteaux et al. 2009, Fricke et al. 2016).

In parallel with the development and sophistication of ultrasonographic examinations in the field of reproduction, a number of clinical conditions have emerged for which ultrasonography has been evaluated for its potential aid as a complementary imaging diagnostic tool. Over time, numerous research studies and growing expertise have resulted in diversification of ultrasound use in cattle leading to the recognition of its diagnostic utility for various indications, including examinations of musculoskeletal structures in cases of lameness, joint instability or penetrating wounds, among others (Flückiger 1997, Buczinski 2009a, Kofler 2009, Braun and Attiger 2016, Re et al. 2016b).

Ultrasonographic evaluation of musculoskeletal structures is facilitated by the superficial location of a majority of them. Consequently, **most rectal probes (transducers) employed today for ultrasonography of the reproductive system can also be utilized for the evaluation of musculoskeletal structures**. Since most practitioners are already equipped with ultrasound units, they do not have to pay additional costs for acquisition of new probes. Another important advantage of ultrasonography is its portability, allowing for musculoskeletal examinations to be performed directly on the farm (Ollivett and Buczinski 2016).

Like any other diagnostic imaging tool, it is important to understand the physical principles responsible for generating ultrasound images and commonly encountered artifacts

(Kirberger 1995, Blond and Buczinski 2009). Understanding how artifacts occur can help their avoidance whenever possible or to use them advantageously to document the nature of the tissues from which they originate (e.g. gas in an abscess, osteophytes, dystrophic mineralization within a tendon, etc.). A few parameter settings that optimize image quality will also be briefly discussed. Therefore, the aim of this introductory chapter is to provide the reader with a brief overview of these important topics.

1.2 Physics and acoustic principles

Ultrasound consists of high frequency vibrations generated by the crystals within a probe. When subjected to an electric field, the crystals inside the probe become excited, which triggers a movement or vibration, generating the emission of the ultrasound wave. This phenomenon is based on the inverse piezo-electric effect of certain materials. The speed at which transmitted ultrasound waves are propagated through a structure of interest varies according to the type of medium.

The speed of ultrasound waves through soft tissues is generally constant at approximately 1,540m/s (Blond and Buczinski 2009).

A wave can be **transmitted** through a medium, as well as **reflected, refracted and attenuated**. Other types of effects such as **diffraction, polarization, dispersion and interference** can also occur.

The interference effect mentioned above is of particular interest for ultrasound examinations that are performed in the proximity of other wave-generating materials or electronic devices, such as ventilation fans in a barn (Kirberger 1995, Blond and Buczinski 2009, Hindi et al. 2013).

A transducer (probe) emits ultrasound waves for only a very small fraction of the time (<0.1%). The remaining time (99.9%) is devoted to reception of ultrasound echoes

reflected back to the probe from tissues. This returning signal will then be converted electronically to form an ultrasound image (sonogram). As a general concept, the time interval between the emission of ultrasound waves and their return as echoes is used to estimate the depth of a specific structure. Information derived from returning echoes and their depth estimation is converted into different shades of white/grey pixels over a black background, generating an image that can be displayed on an ultrasound monitor.

Tissues commonly encountered during ultrasonography of the musculoskeletal system include articular components (capsule, synovial cavities, articular cartilage, menisci), tendons, muscles, ligaments and bones. Although most of these tissues are considered to comprise “soft tissues”, with the exception of bones, they have slightly different acoustic properties that will in turn influence the speed of propagation of ultrasound waves and the behavior of these waves as they travel through different types of media. ▶ Fig. 1-1 summarizes the basic principles of ultrasound propagation within a tissue consisting of two different media (ex: muscle/tendon interface).

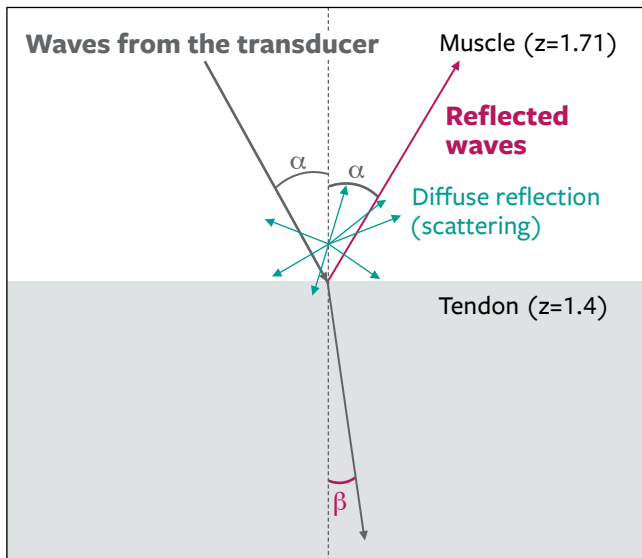


Fig. 1-1: Schematic image of ultrasound propagation characteristics: When a probe is applied over an interface between two tissues of different acoustic impedances, such as a muscle-tendon interface, the ultrasound waves emitted by the transducer strike the interface at an angle alpha (α). Since the impedance difference (z) between these two media is very small, a portion of the emitted ultrasound waves is reflected back to the probe at the same angle as the incident angle. A significant part of the waves is transmitted within the tendon at a refraction angle beta (β). Scattering generally occurs when ultrasound waves strike a diffuse reflector such as blood cells or an irregular organ surface.

1.2.1 Specular reflection

Specular reflection is defined as the mechanism by which ultrasound waves, after encountering a smooth surface, return back to the probe in one direction (Hindi et al. 2013). Indeed, when the incidence of the ultrasound beam strikes a surface with an angle other than perpendicular, the waves can then be reflected with a similar angle (α), but in an opposite direction (▶ Fig. 1-2). The probe would, in turn, not receive any echoes and therefore, no image would be obtained. When a reflected wave actually reaches the probe, then the image of this point will be falsely represented due to the angles of reflection. Reflection only occurs when ultrasound waves reach an interface between two tissues with different acoustic characteristics (or impedance [Z]). Each tissue is characterized by a unique impedance measured in Rayl (for Dr. Rayleigh) equivalent to a unit in $kg/(s \times m^2)$ (Bushberg et al. 2012). ▶ Tab. 1-1 summarizes the impedance of musculoskeletal tissues of interest examined with ultrasound (Sanches et al. 2012).

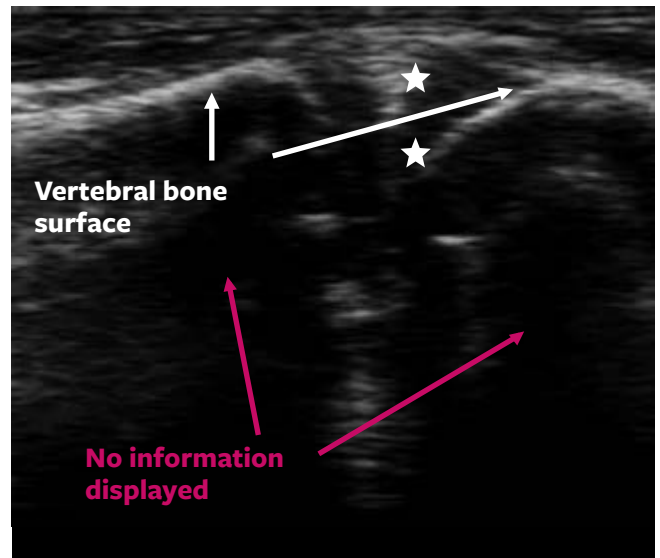


Fig. 1-2: Specular reflection associated with the bone/soft tissue interface: Transrectal sonogram of the lumbosacral joint of an adult Holstein cow with schematic interpretation. The ventral borders of both vertebrae are represented by the hyperechoic lines (**white arrows**). When ultrasound waves strike the soft tissue/bone interface, the high difference in impedance between the two tissues results in their reflection back to the probe. Consequently, there is no information from the deeper parts of the vertebrae and no image can be obtained distal to the vertebral hyperechoic borders. The intervertebral disc space and joint are illustrated (**white stars**).

Tab. 1-1 Impedance of tissues encountered in musculoskeletal ultrasound

Tissue	Impedance* ($\times 10^6$ Rayl)
air	0.0004
fat	1.34
blood	1.65
muscle	1.71
cartilage	1.84
tendon	1.4
bone	7.8

* The impedance values have been reproduced from human references (Sanches et al. 2012).

1.2.2 Diffuse reflection (scattering)

In contrast to specular reflection, diffuse reflection (scattering) occurs when ultrasound waves strike irregular or “rough” surfaces, allowing low amplitude reflection in multiple directions. This type of reflection also leads to attenuation of the ultrasound waves that are transmitted deeper into the tissues.

1.2.3 Attenuation

Attenuation of ultrasound waves, with reflection and refraction, constitutes an important component of image generation in ultrasonography. It is defined as a decrease in the

amplitude of the ultrasound beam as it travels through a medium. Attenuation is influenced by absorption of wave energy by the tissue, and therefore varies according to the nature of the tissue. Since attenuation is positively correlated with frequency, high frequency probes will generate higher attenuation and hence permit a lesser maximal depth of examination than low frequency probes. Further, for the same frequency, ultrasound attenuation is lower for liquids (e.g. blood, synovial fluid) than for muscles or other soft tissues (Duck 2002). Attenuation is greater when produced by bones and fibrotic tissue.

The frequency of ultrasound waves emitted by the probe has an important impact on the image quality and its penetration (► Fig. 1-3a, b). High quality diagnostic images have high spatial resolution, which facilitates the ability to distinguish two structures located next to each other as two individual structures.

As a general rule, high frequency acoustic waves are associated with higher resolution, but they are attenuated more rapidly than low frequency waves. Therefore, depth of imaging is greater with low frequency probes, but it comes at the expense of lower resolution (Bushberg et al. 2012).

1.2.4 Axial, lateral and elevational resolution

Resolution is a general term associated with any optical device. The resolution is defined as the minimal distance between two reflectors allowing for a distinct echo to be returned back to the probe. **The resolution is grossly related**

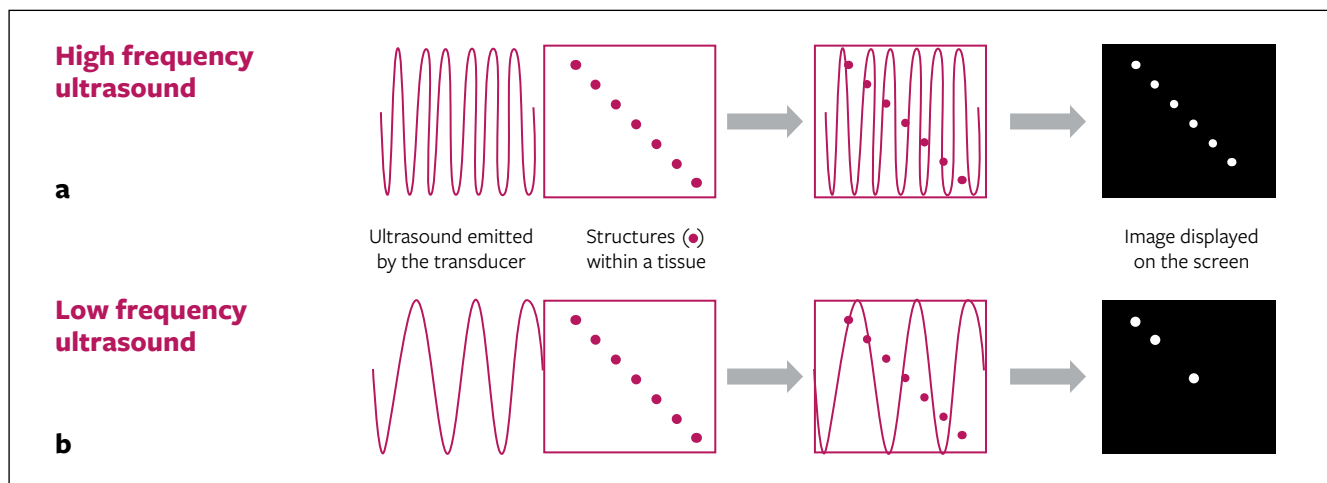


Fig. 1-3a, b: Image quality on using high versus low frequency probes: This figure schematically illustrates the main difference between the capacities of ultrasound waves to discriminate several small structures individually according to their frequencies. The high frequency pulse (a) is able to hit more distinct structures than a low frequency pulse. Consequently, a more detailed image is obtained. In contrast, a low frequency pulse (b) gives a less detailed image, but allows higher wave penetration.

3 Ultrasonographic examination of the distal and proximal interphalangeal joint regions

Maike Heppelmann, Alexander Starke, Johann Kofler

3.1 Introduction

Disorders involving the synovial structures of the distal digit are a common cause of lameness in dairy and beef cattle. Septic arthritis is the most common disease involving the distal (DIJ) and proximal interphalangeal joints (PIJ) (Köstlin and Nuss 1988, Pejsa et al. 1993, Kofler 1995a, Dirksen 2006, Kofler et al. 2007a, Starke et al. 2007a, Burgstaller and Kofler 2016). However, there is evidently a much higher prevalence for infections of the DIJ (Desrochers et al. 1995, Heppelmann et al. 2009a, b, Chamorro et al. 2019). In a study conducted at a Veterinary teaching hospital in cattle with orthopaedic disorders, the ten-year incidence of PIJ infection was 2.4 % and that of DIJ infection was 22.8 % (Kofler 1995a). Similarly, of 85 cattle that required claw amputation because of infection, the DIJ was affected in 32 cases, whereas only six cases involved the PIJ (Pejsa et al. 1993).

The incidences of DIJ and PIJ infection vary because of a difference in the pathogenesis of the disease at each location. Infection of the DIJ usually results from complicated claw disorders, such as sole ulcer, white line disease and interdigital phlegmon, which spread to deeper structures of the claw. Most of these cases are characterised by a communicating tract between the primary claw lesion and the DIJ, whereas septic DIJ infections resulting from penetrating injuries or hematogenous spread of infection are less common (Köstlin and Nuss 1988, Kofler et al. 2007a, Heppelmann et al. 2009a, b, Chamorro et al. 2019).

Septic arthritis of the PIJ usually results from penetrating wounds at the level of the joint pouches or from ascending interdigital phlegmon, or in rare instances it may be acquired by hematogenous spread (Kofler 1995a, Burgstaller and Kofler 2016, Nuss et al. 2019a). Septic arthritis of the PIJ is often accompanied by infection of other synovial structures of the digit, such as the DIJ and/or the close adjoining digital flexor tendon sheath (Hund et al. 2020). One potential source of infection results from communication between the PIJ and

the digital flexor tendon sheath, which may exist rarely in some cattle (Peters 1965). In fact, of eleven cattle with septic arthritis of the PIJ, the infection was limited to this joint in only six cases (Kofler 1995a).

The main differential diagnoses of infection of the DIJ and PIJ include infection of close adjoining synovial structures, such as the digital flexor tendon sheath (► Chap. 11), the fetlock joint (► Chap. 4) and phalangeal fractures. Epiphysitis and osteitis of the phalanges, interphalangeal joint arthrosis (older cows and breeding bulls) and subluxation and distortion are less common (Fischerleitner and Stanek 1987, Kofler 1995a, Nuss et al. 2018, Nuss et al. 2019a, b, Hund et al. 2020).

3.2 Indications for ultrasonographic examination

Ultrasonographic examination of the DIJ/PIJ regions is indicated in cattle with diffuse swelling of the digit when differentiation of the affected structures is not possible by clinical examination alone and/or when there is suspected involvement of multiple synovial structures, including the DIJ and PIJ, one or both digital flexor tendon sheaths or the fetlock joint. An ultrasonographic diagnosis reduces or eliminates the need for arthrocentesis, which carries the risk of joint infection, particularly when the needle is passed through infected tissue. When indicated, arthrocentesis should be performed after ultrasonographic examination because the latter allows for preliminary assessment of the accurate location of liquid joint effusion. This is of practical importance in cases in which arthrocentesis is not successful, for instance in fibrinous arthritis. In addition, arthrocentesis often results in pneumarthrosis, which can severely impede subsequent ultrasonographic examination (Kofler 2009). Most importantly, ultrasonography allows for safe and targeted (indirect) ultrasound-guided arthrocentesis (Heppelmann et al. 2009a, Starke et al. 2009, Kofler et al. 2014).

3.3 Anatomy

The DIJ is a saddle joint that primarily accommodates extension and flexion. The joint is formed by the distal articular surface of the middle phalanx (P2), the articular surface of the distal phalanx (P3) and the articular surface of the distal sesamoid bone. Its dorsal pouch extends proximally along P2 to approximately 2 cm above the coronet near the dorsal pouch of the PIJ and is superimposed by the common digital extensor tendon. At the palmar/plantar aspect, the pouch of the DIJ extends along P2 to just below the flexor tuberosity of P2 and is bounded on the palmar/plantar aspect by the deep digital flexor tendon sheath (► Fig. 3-1) (Stanek 1987, Dyce et al. 2002, Nickel et al. 2004a, König and Liebich 2014, Maierl et al. 2019).

The PIJ is also a saddle joint, which is formed by the distal articular surface of the proximal phalanx (P1) and the proximal articular surface of P2 and allows predominantly flexion and extension of the joint. Dorsally the joint pouch extends 2–3 cm proximally, and distally it extends mostly axi-

ally along P2 to the region of the pouch of the DIJ. The pouch is superimposed dorsally by the two digital extensor tendons. Abaxially, the pouch of the PIJ extends proximally above the middle of P1 where it is bordered by the digital flexor tendon sheath (► Chap. 11). The palmar/plantar pouch of the PIJ is located dorsally of the digital flexor tendon sheath and extends proximally one third of the length of P1 (► Fig. 3-1) (Stanek 1987, Dyce et al. 2002, Nickel et al. 2004a, König and Liebich 2014, Maierl et al. 2019). In rare cases, there is communication between the PIJ and the digital flexor tendon sheath of the pelvic limbs (Peters 1965).

3.4 Ultrasonographic examination procedure and anatomical landmarks

Ultrasonographic examination of the DIJ and PIJ regions can be carried out in standing cattle. However, it is highly recommended that the examination is performed in a restrained animal in a chute with the limb securely lifted or on the restraint animal in lateral recumbency on a tilt table. For personal safety reasons and to protect the ultrasound equipment from damage, the limb to be examined should always be secured. Sedation of the animal may be required. The region of interest is clipped or shaved, and the skin is cleaned with water. Then liberal amounts of acoustic coupling gel are applied to the skin and the probe.

Linear probes with a frequency of 7.5 to 12 MHz are suitable for imaging the dorsal, lateral and palmar/plantar aspects of the DIJ and PIJ regions because in most cases the structures of interest are located within 1–5 cm of the skin surface (Heppelmann et al. 2009a, Kofler 2009, Kofler 2011, Gonçalves et al. 2014, Kofler et al. 2014, Chapuis et al. 2020).

The **standard examination plane of choice for imaging the DIJ and the PIJ** is the longitudinal plane with the probe placed on the dorsal and palmar/plantar aspects of the digit proximal to the coronary band. Imaging of the structures from the palmar/plantar aspect in the longitudinal plane is sometimes difficult, in particular in adult cattle, because of folding of the skin between the dew claws and the bulbs of the heel and the frequent occurrence of swelling in the heel region, which makes good contact between the (too long) linear probe and the skin nearly impossible (Heppelmann et al. 2009a, Kofler 2009, Kofler et al. 2014).

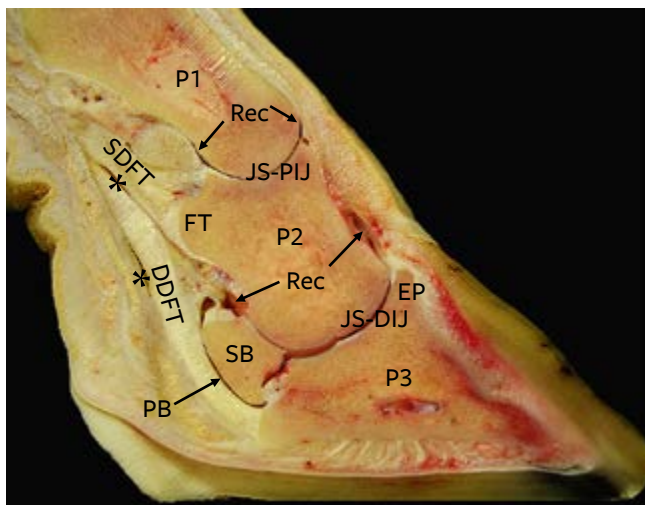


Fig. 3-1: Sagittal anatomical section of a normal hind digit of a cow showing all the relevant structures: the joint space of the distal (**JS-DIJ**) and the proximal interphalangeal joint (**JS-PIJ**), the dorsal and plantar joint pouches (**Rec**) of DIJ and PIJ; proximal phalanx (**P1**), middle phalanx (**P2**), distal phalanx (**P3**), extensor process (**EP**) of P3, distal sesamoid bone (**SB**), podotrochlear bursa (**PB**), superficial digital flexor tendon (**SDFT**) with its insertion at the flexor tuberosity (**FT**) of P2, deep digital flexor tendon (**DDFT**), and small normal lumen of the digital flexor tendon sheath (*).

ANATOMICAL LANDMARKS

The anatomical landmarks for ultrasonographic examination of the PIJ and DIJ are:

- the joint space of the PIJ between the proximal and middle phalanx,
- the joint space of the DIJ between the middle and distal phalanx,
- the bone surfaces of the proximal and middle phalanx, the extensor process of the distal phalanx and the distal sesamoid bone,
- the flexor and extensor tendons.

The following structures of the PIJ and DIJ regions should be evaluated ultrasonographically (Kofler and Edinger 1995, Tryon and Clark 1999, Heppelmann et al. 2009a, Kofler 2009, Kofler 2011, Gonçalves et al. 2014, Kofler et al. 2014):

1. **joint space, joint capsule and dorsal and palmar/plantar joint pouch of the PIJ** using the longitudinal plane over the dorsal and palmar/plantar aspect of the PIJ;
2. **joint capsule and dorsal and palmar/plantar joint pouch of the DIJ** using the longitudinal plane: the dorsal and palmar/plantar aspects, proximal to the coronary band;
3. **the maximum dorsopalmar/-plantar dimension of the dorsal joint pouch** of the DIJ and the PIJ using the longitudinal plane for diagnosis of septic arthritis;
4. **bone surfaces** of the phalangeal bones (P1, P2, P3) and the distal sesamoid bone: echogenicity and characteristics of the bone surfaces using the longitudinal (and transverse) planes on the dorsal and palmar/plantar aspects;
5. superficial and deep digital flexor **tendons** and common and lateral digital extensor tendons with their **tendon sheaths**: the dorsal and palmar/plantar aspects in transverse and longitudinal planes (► Chap. 11).

3.5 Normal ultrasonographic appearance of the anatomical structures

The normal ultrasonographic appearance of the anatomical structures of the bovine musculoskeletal system is listed in ► Tab. 2-1 (► Chap. 2). In the longitudinal plane, the dorsal

bone surfaces of P1 and P2 appear as slightly curved, smooth and hyperechoic lines. The joint space of the PIJ appears as a small anechoic interruption of the bone contour similar to a stylized seagull (► Fig. 3-2a-c) (Kofler and Edinger 1995, Tryon and Clark 1999, Heppelmann et al. 2009a, Gonçalves et al. 2014). The joint space of the normal DIJ could be visualised only rarely in adult cows because it is located within the horn capsule (Kofler and Edinger 1995, Heppelmann et al. 2009a), but has been imaged in healthy six-month-old Girolando calves together with the proximal part of P3, the extensor process (Gonçalves et al. 2014). The distal sesamoid bone is imaged at the palmar/plantar aspect as a slightly convex, smooth and hyperechoic contour close to the skin surface (► Fig. 3-2a-c).

The joint capsules of the PIJ and DIJ appear as thin echoic structures immediately adjacent to the joint surface (Gonçalves et al. 2014). The normal dorsal and palmar/plantar pouch of the PIJ cannot be visualised (► Fig. 3-2a-c) (Kofler and Edinger 1995). In the longitudinal plane, the dorsal pouch of the DIJ appears as an elongated, semicircular structure that runs proximally along the dorsal aspect of P2 (► Fig. 3-2a-c). In healthy adult cows, the maximum dorsopalmar/-plantar dimension of the dorsal joint pouch of the DIJ is 4.1 mm (± 0.7). The normal dorsal joint pouch of the DIJ appears as a small anechoic area. The echogenicity of the normal dorsal joint pouch of the DIJ may be sometimes higher (hypoechoic or echoic) so that it does not differ from that of a septic joint (Heppelmann et al. 2009a). This phenomenon is based on a noise artifact caused by the proximity of the structures to the probe (Kirberger 1995), and has to be kept in mind to avoid misinterpretation. Provided that there is optimal contact between the probe and the skin between the dew claws and coronary band, the palmar/plantar pouch of the DIJ can be visualised dorsal of the deep digital flexor tendon as a semicircular area that appears hypoechoic relative to the surrounding tissues (► Fig. 3-2a-c).

The common and lateral digital extensor tendons appear as echoic bundles of parallel fibres located directly under the skin (Gonçalves et al. 2014). Provided there is optimal contact between the probe and skin between the dew claws and coronary band, the superficial and deep digital flexor tendons, surrounded by the distal compartment of the digital flexor tendon sheath, can be visualised in the longitudinal (► Fig. 3-2b, c) and transverse planes (► Chap. 11).

3 Ultrasonographic examination of the distal and proximal interphalangeal joint regions

3

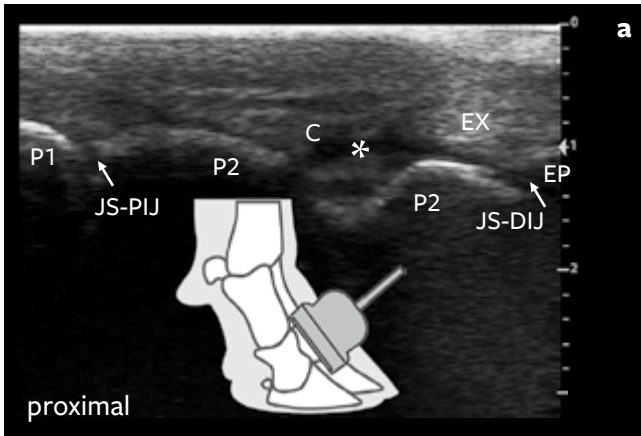


Fig. 3-2a: Longitudinal sonogram (5.0 MHz linear) of the dorsal aspect of a healthy bovine digit of a six-month-old Simmental heifer showing the joint spaces of distal (**JS-DIJ**) and proximal interphalangeal joints (**JS-PIJ**); the normal small dorsal pouch of the PIJ cannot be differentiated, the normal small dorsal pouch of the DIJ is indicated by a small anechoic area (*), joint capsule (**C**); smooth hyperechoic dorsal contour of proximal (**P1**) and middle phalanx (**P2**); extensor tendon (**EX**) inserting at the extensor process (**EP**) of the distal phalanx.

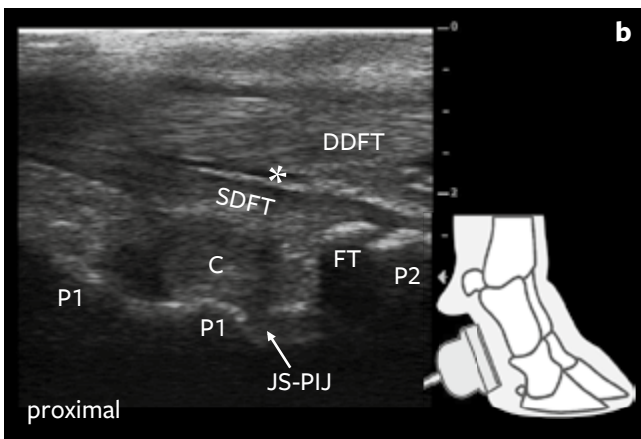


Fig. 3-2b: Longitudinal sonogram (5.0 MHz linear) of the plantar aspect of a healthy bovine digit of the same heifer showing the smooth hyperechoic plantar contour of P1 and P2, the joint space (**JS-PIJ**) in-between, deep digital flexor tendon (**DDFT**), superficial digital flexor tendon (**SDFT**) with its insertion at the flexor tuberosity (**FT**) of P2. The small anechoic area (*) indicates the normal amount of synovial fluid in the digital flexor tendon sheath; the plantar joint capsule (**C**) and the plantar joint pouch cannot be differentiated.

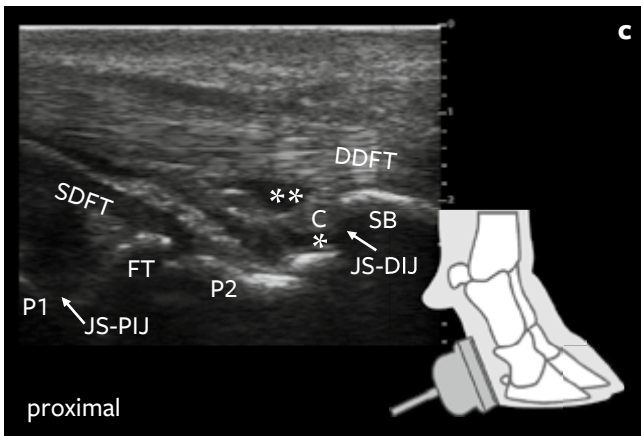


Fig. 3-2c: Longitudinal sonogram (5.0 MHz linear) of the distal plantar aspect of a healthy bovine digit of the same heifer showing the smooth hyperechoic plantar contour of P1 and P2, the distal sesamoid bone (**SB**), both joint spaces (**JS-PIJ**, **JS-DIJ**), the deep digital flexor tendon (**DDFT**), superficial digital flexor tendon (**SDFT**) with its insertion at the flexor tuberosity (**FT**) of P2. The small anechoic area (*) indicates the normal amount of synovial fluid in the DIJ and the joint capsule (**C**) of DIJ. The small anechoic area (**) indicates the normal amount of synovial fluid in the proximal part of the podotrochlear bursa (**).

3.6 Sonopathological findings

Common ultrasonographic findings in cases of septic (rarely aseptic) arthritis of the DIJ and the PIJ and septic osteitis and osteomyelitis of the joint-forming bones have been described (Kofler 1995a, Heppelmann et al. 2009a, Kofler 2009, Kofler 2011, Kofler et al. 2014, Burgstaller and Kofler 2016, Nuss et al. 2019b).

3.6.1 Arthritis of the DIJ

Septic arthritis of the DIJ is always associated with distension (► Fig. 3-3 to 3-6) of the dorsal (and palmar/plantar) joint pouch (Kofler and Edinger 1995, Kofler et al. 2007a, Starke et al. 2007a, Heppelmann et al. 2009a, Nuss et al. 2019b). Ultrasonographic examination of the dorsal joint pouch is the diagnostic method of choice because folding of the skin between the dew claws and the bulbs of the heel and/or moderate to severe swelling of the heel bulbs have been shown to impair visualisation of the palmar/plantar joint pouch of the DIJ in 54 % of cattle with septic arthritis (Heppelmann et al. 2009a). The maximum dorsopalmar/-plantar dimension of the dorsal joint pouch was measured in the longitudinal plane approximately 1 cm axial to the midline of the digit (► Fig. 3-3 to 3-6). At this location the sensitivity and specificity of a measurement greater than the threshold value of 6 mm for

the diagnosis of septic arthritis of the DIJ exceeds 0.95 in adult cows. The echogenicity of the effusion of the dorsal pouch of the DIJ has low specificity and sensitivity for the diagnosis of septic arthritis, partly because hypoechoic joint fluid seen in septic arthritis may also be observed in a normal DIJ. Hemarthrosis should be included in the differential diagnosis when the joint fluid is homogeneously hypoechoic (Heppelmann et al. 2009a).

Inducible flow phenomena were visualised in 30 % of DIJs with septic arthritis (Heppelmann et al. 2009a). This variable had a high specificity (1.0) for diagnosis of septic arthritis of the DIJ because flow phenomena could not be induced in normal DIJs. However, the sensitivity of this variable was low at 0.3.

Based on the specific aetiology, a communication channel between the joint pouch and a sole defect (sole ulcer, white line lesion) is common in cases of septic arthritis of the DIJ. Interestingly, this does not seem to have a significant effect on the dorsopalmar/-plantar dimension of the dorsal joint pouch and thus on the ultrasonographic visibility of joint effusion (Heppelmann et al. 2009a).

Arthrocentesis of the dorsal pouch of the DIJ is performed approximately 1 cm proximal to the coronet, axially or abaxially to the common digital extensor tendon in a slightly distal direction (Desrochers et al. 2001, Nuss et al. 2002a, Heppelmann et al. 2009a, Kofler 2018).

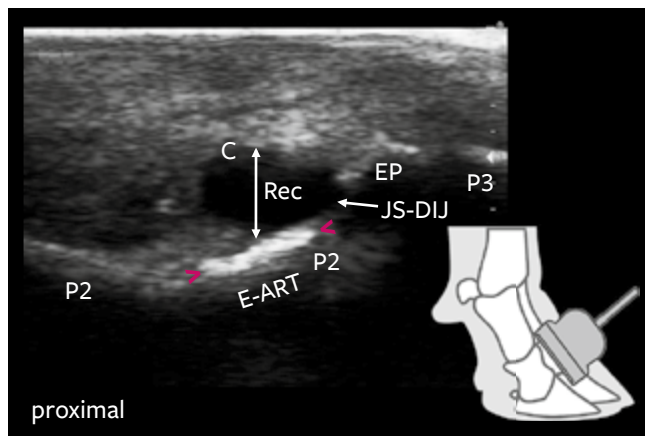


Fig. 3-3: Longitudinal sonogram (5.0 MHz linear) of the dorsal aspect of the distal digital region of a 3.5-year-old Simmental cow with septic serous arthritis of the DIJ resulting from a white line abscess; the **white arrow** demarcates the dorsoplantar width (approximately 6.6 mm) of the distended dorsal pouch (**Rec**) showing an anechoic effusion; therefore an enhancement artifact (**E-ART**) can be seen directly distally (**between the pink arrows**), depicting this particular part of the smooth dorsal bone contour of the middle phalanx (**P2**) much more hyperechoic as the same bone contour more proximally; the joint capsule (**C**), the joint space of the DIJ (**JS-DIJ**) and the extensor process (**EP**) of distal phalanx (**P3**).

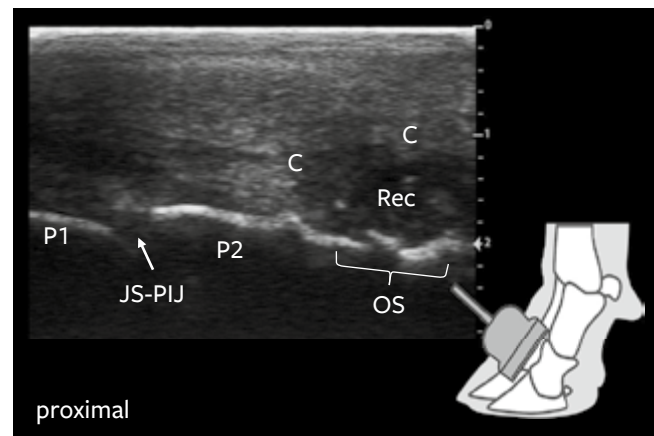


Fig. 3-4: Longitudinal sonogram (5.0 MHz linear) of the dorsal aspect of the distal digital region of a 3.5-year-old Aberdeen Angus cow with purulent arthritis of the DIJ and bone infection resulting from an interdigital phlegmon. The distended dorsal pouch (**Rec**) shows a heterogeneous effusion, joint capsule (**C**), smooth hyperechoic dorsal contour of the proximal phalanx (**P1**) and of the proximal contour of the middle phalanx (**P2**), joint space of PIJ (**JS-PIJ**); the irregular and rough distal contour of P2 indicates osteolysis (**OS, bracket**).

7 Ultrasonographic examination of the shoulder region

Birgit Altenbrunner-Martinek, Karl Nuss, Alexander Starke, Johann Kofler

7.1 Introduction

Disorders of the bovine shoulder and scapular region have been rarely reported in cattle, and are usually unilateral and only affect individual animals (Buergelt et al. 1996). Septic or aseptic arthritis of the shoulder joint may be difficult to diagnose exclusively by clinical examination (Desrochers et al. 2001, Nuss 2003, Desrochers and Francoz 2014, Kofler et al. 2018). Scapulohumeral arthritis, bursitis of the infraspinous and the bicipital bursae, fractures of the scapula and scapulohumeral luxation are responsible for most shoulder lameness (Tulleners et al. 1985, Ferguson 1997, Nuss 2000, Dirksen 2006). All of these disorders are clinically characterized by swing-phase lameness, a localized or diffuse swelling of the shoulder region and a painful response to palpation. Direct evaluation of the joint pouch by palpation is not possible due to its location some centimeters under the skin surface (Desrochers et al. 2001, Kofler et al. 2018).

Over the last few years, ultrasonography has been widely used for diagnosis of joint, tendon, ligament and muscle disorders in cattle, but also for diagnosing bone lesions such as fractures, luxation, fissures, bone sequestration and osteomyelitis involving the growth plates (Nuss 2000, Kofler 1996a, Kofler 1997a, Nuss et al. 2007, Starke et al. 2008, Nuss et al. 2018). In particular, in cattle, where diagnostic imaging of the shoulder joint with other modalities such as radiography, computed tomography or magnetic resonance imaging is usually not practical, ultrasonography should be used as the standard examination tool in clinics and practice (Nuss 2003, Kofler 2009, Kofler et al. 2014, Altenbrunner-Martinek et al. 2017, Nuss et al. 2018).

7.2 Indications for ultrasonographic examination

Ultrasonographic examination of the shoulder is always indicated for differentiation of any soft tissue swelling located in this region (Nuss 2003, Nuss et al. 2007, Kofler 2009, Kofler 2011, Kofler et al. 2014, Altenbrunner-Martinek et al. 2017).

Clinically evident swelling of the shoulder region, combined with localized pain and lameness as leading symptoms, can be seen in cases with septic or aseptic arthritis, bursitis of the infraspinous bursa and/or the bursa underlying the biceps tendon respectively, periarticular abscesses and hematomas, lesions of the lateral shoulder muscles – that serve as collateral ligaments in this area – and other muscles located in this region or bone lesions including osteomyelitis of the growth plates of the distal scapula, the greater tubercle and the humeral head, articular subchondral bone infection, fractures of the scapula or the proximal aspects of the humerus and luxation of the scapulohumeral joint (Ferguson 1997, Dirksen 2006, Nuss et al. 2007, Kofler et al. 2016, Altenbrunner-Martinek et al. 2017).

7.3 Anatomy

The shoulder joint is composed of the junction of the distal end of the scapula (glenoid cavity) with the proximal end of the humerus. The large tendons of the infraspinous and supraspinous muscles laterally, the subscapularis muscle medially and the biceps brachii muscle cranial of the shoulder joint region serve as functional “collateral” ligaments in the absence of proper collateral ligaments. The bicipital (intertubercular) bursa lies between the humeral tubercles cushioning the bicipital tendon (► Fig. 7-1a, b). The supraspinous muscle is covered by the trapezius, omotransverse muscle and brachiocephalicus muscles. The supraspinous muscle originates from the supraspinous fossa and inserts with a larger branch at the greater tubercle and with a smaller branch at the minor tubercle of the humerus. These two branches have a predominantly tendinous character.

The infraspinous muscle originates at the scapular spine and the infraspinous fossa of the scapula, crosses the shoulder joint space laterally and inserts with a deeper located muscular branch on the lateral aspect of the greater tubercle. The superficial tendinous part crosses the proximal rim of the greater tubercle and the subtendinous infraspinous bursa as a firm and flat tendon and inserts on the lateral part of



Fig. 7-1a, b: Longitudinal anatomical section (transected in a craniolateral-caudomedial plane) (a) of the shoulder joint region of a five-month-old calf showing some important anatomical structures of the scapulohumeral joint: the greater tubercle (GT) of the humerus, humeral head (HH), humerus (HU), cartilaginous growth plate (*) between the greater tubercle and humerus and the humeral head respectively, the joint space (JS), scapula (SC), glenoid tubercle of the scapula (SGT), normal joint pouch (Rec), cartilage (Ca-GT) covering the greater tubercle, articular cartilage (Ca), supraspinous muscle (SM) and the deltoid muscle (DM).

Longitudinal anatomical section of the shoulder joint region of a six-month-old calf (b) showing the course of the bicipital tendon running over the greater tubercle (GT); the bicipital tendon (BT), lumen of the bicipital bursa (black arrows), biceps brachii muscle (BBM), deltoid muscle (DM), fatty tissue (F), cartilaginous growth plate (*) between greater tubercle and humerus (HU) and skin (S).

the greater tubercle. The proximal rim of the scapular bone carries the strong, crescent-shaped scapular cartilage, which can be palpated in skinny animals (Dyce et al. 2002, Nickel et al. 2004a, König and Liebich 2014, Wünsche et al. 2011).

7.4 Ultrasonographic examination procedure and anatomical landmarks

Before starting the ultrasonographic examination of the shoulder region, adult cattle should be restrained in a crush and preferably should be scanned in the standing position. Alternatively, this region can also be examined in the animals restrained on a hydraulic tilt table in lateral recumbency with the affected limb placed at the top. Calves can be examined in the standing position while fixed by the head and hips. Usually, sedation is not necessary. The shoulder joint region should be clipped, and the skin washed and cleaned with water. Afterwards a generous quantity of coupling gel is applied. The use of a standoff pad is not recommended.

The 7.5 MHz linear probe (5–8 MHz multifrequency linear probe) is recommended for calves, as it enables imaging of all aspects of the shoulder region. For examination of the biceps tendon at the cranial part of the shoulder region in adult cattle a 3.5–5 MHz convex probe should be used, because correct positioning of a linear probe for the examination of the biceps tendon is impeded by the prominent greater tubercle. **All other structures in adult cattle can be visualized by the use of a 5–8 MHz linear multifrequency probe or alternatively by a 3.5–5 MHz convex probe.** All the accessible structures of the cranial and lateral aspects of the shoulder region should be scanned in both longitudinal and transverse planes, beginning cranioproximally and moving stepwise distally and caudally (Altenbrunner-Martinek et al. 2007, Kofler 2009, Chapuis et al. 2020).

ANATOMICAL LANDMARKS

The anatomical landmarks for ultrasonographic examination of the shoulder joint region are:

- the scapular spine,
- the scapulohumeral joint space,
- the greater tubercle of the humerus and
- the biceps and infraspinatus tendons.

The standard examination planes of choice for imaging the most important anatomical structures of the shoulder joint region are (Altenbrunner-Martinek et al. 2007, Kofler 2009, Kofler et al. 2014):

1. the longitudinal plane over the lateral aspect of the shoulder joint region directly below the scapular spine; this view allows imaging of the joint space, the bone surfaces of the distal part of the scapula and the humeral head, the infraspinous fossa and the two branches of the infraspinous muscle, the insertion of the tendinous part of the infraspinous muscle at the lateral surface of the humerus with the underlying bursa, and the cartilaginous growth plate of the glenoid tubercle of the scapula (close to the glenoidal cavity) and the growth plate between the humeral head and the proximal humerus in calves;
2. the longitudinal plane on the craniolateral aspect of the shoulder joint that permits imaging of parts of the joint space and the cranial portion of the joint pouch, the greater tubercle with its two parts and the cartilaginous growth plates between the humerus and the greater tubercle in calves;
3. the transverse plane (preferably) on the cranial aspect of the shoulder joint to depict the biceps tendon and the bicipital bursa, starting from its origin at the supraglenoid tubercle.

The following anatomical structures of the shoulder joint region should be examined ultrasonographically (Nuss 2003, Altenbrunner-Martinek et al. 2007, Kofler 2009, Kofler et al. 2014, Chapuis et al. 2020):

1. **joint space, joint recess and joint capsule** in longitudinal planes at the craniolateral, lateral and laterocaudal aspects of the shoulder joint;
2. **scapular spine, supraspinous and infraspinous fossa, distal part of the scapula, greater tubercle, humeral head, articular cartilage and subchondral bone:** noting echogenicity and appearance of the bone surfaces in the transverse plane at the lateral aspects of the scapula for the scapular spine, the supraspinous fossa and the infraspinous fossa and then the longitudinal plane starting craniolaterally for the greater tubercle and moving laterally for the joint-forming parts of the scapula and humerus (glenoidal cavity, humeral head and greater tubercle);
3. **cartilaginous growth plates** of the glenoid tubercle of the scapula, between the greater tubercle and the humeral head, and between the humeral head and the proximal humerus in calves in the longitudinal plane starting craniolaterally at the shoulder joint region and moving the probe stepwise to the laterocaudal aspect;

4. **bicipital bursa** in the transverse plane at the cranial aspect of the shoulder joint, and **infraspinous bursa** laterally in the longitudinal and transverse plane; examination of the biceps tendon in adult cattle is preferably performed in the transverse plane due to the prominent major tubercle. However, the origin of the biceps tendon at the supraglenoid tubercle can be identified more easily in the longitudinal plane;
5. **muscles** at the lateral aspect (supraspinous muscle covered by the trapezius muscle, omotransverse muscle and brachiocephalicus muscle and the two branches of the infraspinous muscle) and cranial muscles (biceps brachii muscle with its tendon) are examined in longitudinal and transverse planes in the search for pathologic alterations (myositis, laceration, abscess, ...).

7.5 Normal ultrasonographic appearance of the anatomical structures

The normal ultrasonographic appearance of the most important anatomical structures of the bovine musculoskeletal system is listed concisely in ►Tab. 2-1, ►Chap. 2.

7.5.1 Scapula and humerus

The outer contours of the scapula and humerus appear as smooth, hyperechoic surfaces with acoustic shadowing distally (►Fig. 7-2a, b). The continuity of the smooth bone surface of the scapula is disrupted by the bony protuberance of the scapular spine (►Fig. 7-2b). The same condition can be seen on the proximal end of the humerus where the normal smooth bone surface is disrupted by the prominence of the greater tubercle. These pseudo-disruptions are normal and should not be mistaken for fractures. When scanned in transverse planes, the scapular spine appears as a hyperechoic reflection of the upper angle of an imaginary triangle, the two lower angles being formed by the supraspinous and infraspinous fossae. The sides of this imagined triangle cannot be seen owing to an acoustic phenomenon caused by the angle of the ultrasound probe in relation to the bone surface (►Fig. 7-2b). The sides of this triangle (the scapular spine) can only be visualized when the angle of the probe is adjusted to this structure by directing it obliquely to the long axis of the extremity. Careful scanning of these structures in transverse and longitudinal planes proves them to be contiguous with the bone surface. In calves, the cartilaginous growth plates of the glenoid tubercle of the scapula and the humerus between the greater tubercle and the humeral head

and respectively the humerus (►Fig. 7-2a, ►Fig. 7-3) can be imaged as small anechoic zones interrupting the hyperechoic bone surfaces. In adult cattle, the surface of the greater tubercle appears hyperechoic with acoustic shadowing distally. In calves, depending on their age, the greater tubercle may consist of a thick cartilaginous layer with a heterogeneous appearance (►Fig. 7-10a, b) interspersed with small echoic spots (Altenbrunner-Martinek et al. 2007, Chapuis et al. 2020).

7.5.2 Scapulohumeral joint, bicipital and infraspinous bursa

In the longitudinal plane, the scapulohumeral joint space appears as a clearly outlined interruption of the hyperechoic bone surfaces of the scapula and the humeral head at the lateral aspect of the shoulder region (►Fig. 7-3, ►Fig. 7-4). In adult cattle, only a small portion of the articular surface at the cranial, lateral and lateral-caudal aspects of the shoulder is accessible for ultrasonographic examination. In calves, examination of a larger portion of the articular surface of the humeral head is possible and can be facilitated by passive movement of the limb during the examination procedure. While in adult cattle the articular cartilage covering the humeral head can be imaged as a thin anechoic (►Fig. 7-4) layer of approximately 1 mm thickness, in calves the articular cartilage shows an anechoic appearance, interspersed with small hypoechoic and echoic spots and is obviously thicker (5 mm and more) than in adults (►Fig. 7-10a).

Normally, the scapulohumeral joint pouch and the bursal cavities can either not be differentiated at all or they can only be seen as small anechoic zones of synovial fluid. The bicipital bursa and the bursa underlying the infraspinatus tendon can only be visualized as a discrete anechoic line. Evaluation or differentiation of the joint capsule of the shoulder joint, the capsules of the infraspinous bursa and the bursa surrounding the biceps tendon is not possible (►Fig. 7-2a, ►Fig. 7-3, ►Fig. 7-4) in healthy shoulder joints (Altenbrunner-Martinek et al. 2007).

7.5.3 Tendons and muscles

The tendon of the biceps muscle can easily be identified. It appears as an echoic structure with a strong linear pattern of parallel fiber bundles in the longitudinal plane. After localisation of the greater tubercle and its adjacent intertubercular (bicipital) groove by digital palpation, the ultrasound probe is positioned perpendicular to this groove to obtain a transverse image of the tendon. In this transverse plane, the biceps tendon can be identified as an oval-shaped,

homogeneous echoic structure. At the muscle-tendon transition a small 'cap' of hypoechoic muscle fibers can be seen cranially attached to the tendon. In the longitudinal plane, the origin of the biceps tendon at the supraglenoid tubercle appears as a cord of small parallel fiber bundles arising from a hyperechoic convex bony structure. Due to the prominent anatomical shape of the greater humeral tubercle in adult cows, examination of the origin of the biceps tendon is rather difficult; the size of the greater tubercle and the anatomical shape complicates the accurate positioning of the ultrasound probe at the correct location.

The supraspinous muscle has a moderate anechoic to hypoechoic echogenicity, interrupted by echoic septa, and can be seen at the supraspinous fossa directly adjoining the hyperechoic bone surface. At the beginning of the bicipital groove the supraspinous muscle with its two branches are wrapped around the biceps tendon. In contrast to adult cattle, where the biceps tendon is oval-shaped and perpendicular to the long axis of the extremity in the transverse plane, in

calves the biceps tendon resembles a teardrop. Caudal to the scapular spine, which can easily be identified by palpation, the infraspinous fossa, which is covered by the two branches of the infraspinous muscle, can be imaged (► Fig. 7-2b). The deeper muscular part of the infraspinous muscle has a hypoechoic appearance with echoic septa and covers the hyperechoic bone surface. The superficial tendinous portion is more homogeneous, echoic and passes over the lateral aspect of the humeral head and the greater tubercle to its insertion at the humeral surface distal of the greater tubercle. In the transverse plane, the infraspinatus tendon has a wide, flat and echoic appearance, whereas in the longitudinal plane this tendon appears as a cord of small parallel fiber bundles (► Fig. 7-3). The deltoid muscle covers the infraspinatus tendon in this area. However, the tendon can be distinguished from the deltoid muscle due to its strong linear pattern of parallel, echoic fiber bundles (Altenbrunner-Martinek et al. 2007, Chapuis et al. 2020).

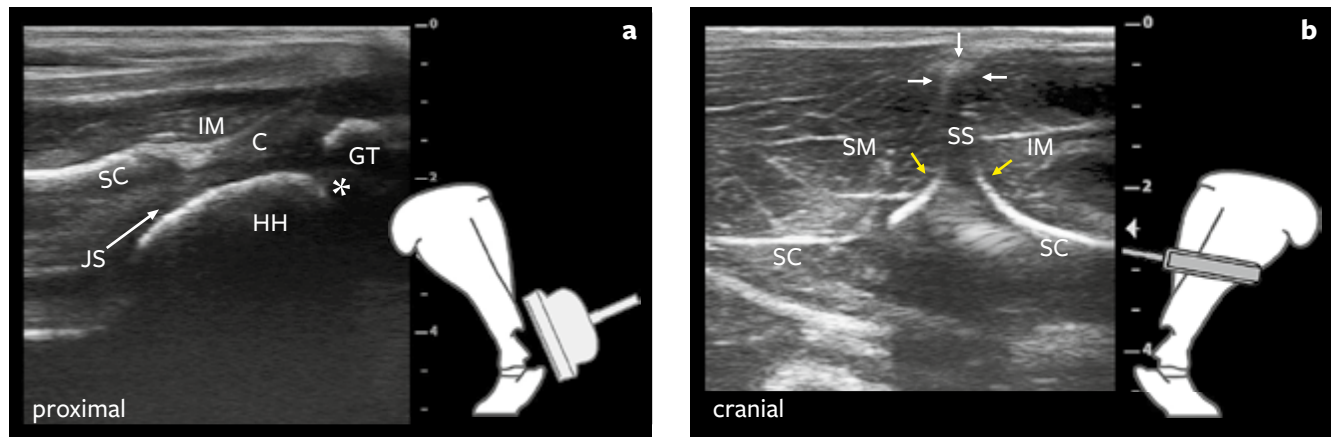


Fig. 7-2a, b: Longitudinal sonogram (7.5 MHz linear) of the laterocaudal aspect (**a**) of the left shoulder joint region in a healthy five-week-old Simmental calf showing the normal appearance of some important structures: normal hyperechoic surface of the scapula (**SC**), scapulohumeral joint space (**JS**), joint capsule (**C**), hyperechoic convex surface of the humeral head (**HH**), hyperechoic convex surface of the greater trochanter (**GT**), the small anechoic interruption in-between represents the cartilaginous growth plate (*); the infraspinous muscle (**IM**) covers these bony structures.

Transverse sonogram (7.5 MHz linear) of the lateral aspect of the scapula (**b**) (taken approximately at its midline) in the same calf showing the normal appearance of the scapular muscles and the scapular surface: the continuity of the normal smooth hyperechoic surface of the scapula (**SC**) is interrupted by the normal protuberance of the scapular spine (**SS**), which is directed more or less parallel to the penetrating ultrasound waves. Therefore, only the very small top (**white arrows**) of the scapular spine (**SS**) can (hardly) be identified as a delicate contour. The cranial and caudal contours of the scapular spine cannot be imaged as ultrasound waves are not reflected by structures structures running parallel to the incident waves. However, at the distal end of the scapular spine, where its bone contours bend into the scapular fossa (**yellow arrows**), the contours become clearly imaged. The supraspinous muscle (**SM**) can be identified cranially and the infraspinous muscle (**IM**) caudally.

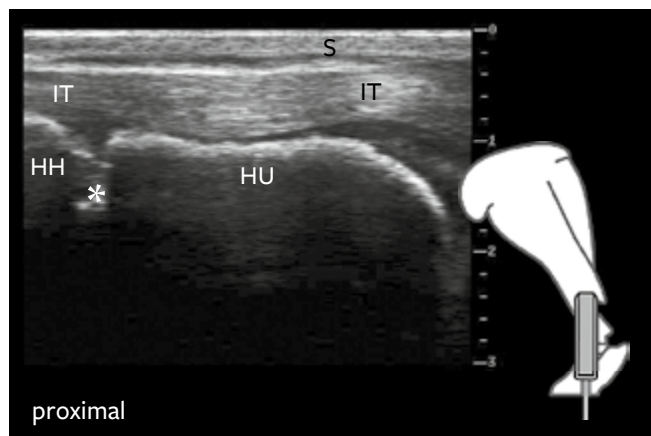


Fig. 7-3: Longitudinal sonogram (7.5 MHz linear) of the lateral aspect of the scapulohumeral joint region of a three-month-old Brown Swiss calf showing the normal infraspinatus tendon (**IT**) characterized by the echoic tendon fiber bundles showing their normal parallel alignment; the lateral contour of the humeral head (**HH**), and the cartilaginous growth plate (*) between the humeral head (**HH**) and the humerus (**HU**); the skin (**S**).

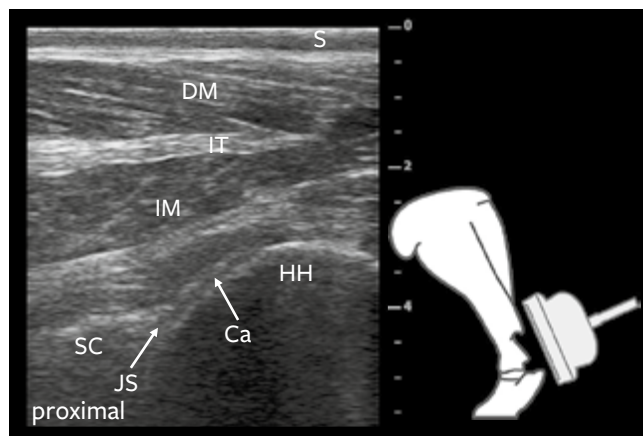


Fig. 7-4: Longitudinal sonogram (5 MHz linear) of the lateral aspect of the shoulder joint region of a six-year-old Simmental cow showing its normal appearance; smooth hyperechoic distal part of the scapula (**SC**), smooth hyperechoic convex surface of the humeral head (**HH**): the scapulohumeral joint space (**JS**) appears as a small funnel-shaped interruption of the hyperechoic bone surfaces. The very small anechoic band covering the convex contour of the humeral head represents the thin articular cartilage (**Ca**). The more superficially located tendinous part (**IT**) of the infraspinatus muscle (**IM**) is characterized by the parallel arrangement of its fiber bundles and an echoic appearance, whereas the deeper muscular part (**IM**) appears more anechoic; the infraspinatus muscle (**IM**) is covered by the deltoid muscle (**DM**) and the skin (**S**).

7.6 Sonopathological findings

The shoulder joint and bursae normally contain only small amounts of synovial fluid so that the joint pouch and the bursal lumen cannot be differentiated at all or only with difficulty (Altenbrunner-Martinek et al. 2007, Chapuis et al. 2020). In cases of inflammation of these synovial cavities, they appear as mildly to severely distended cavities filled with an inflammatory effusion and/or clotted masses of varying echogenicity. Effusions can be detected by ultrasound during the very early stages of synovitis (Nuss 2003, Nuss et al. 2007, Kofler 2009, Kofler 2011, Kofler et al. 2014, Altenbrunner-Martinek et al. 2017).

Osteochondrosis, other degenerative articular changes and subchondral bone lesions, causing lameness and effusion of the scapulohumeral joint, can also readily be diagnosed ultrasonographically (Nuss et al. 2018).

7.6.1 Arthritis

Characteristic for an arthritis of the scapulohumeral joint is the presence of an anechoic to hypoechoic effusion associated with a mildly to severely elevated joint capsule. The echogenicity of the effusion depends on the character of inflammation. Serous effusion has an anechoic appearance, while anechoic effusion containing small hypoechoic spots is a typical finding in serofibrinous arthritis (► Fig. 7-5 to 7-7). In all cases with liquid effusion, flow-phenomena can be assessed with hypoechoic to echoic debris floating in the anechoic fluid. Fibrino-purulent arthritis is associated with a heterogeneous hypoechoic joint effusion caused by clotted gelatinous masses of fibrin and liquid purulent exudate. These heterogeneous semi-solid masses do not allow for clear differentiation of the echoic joint capsule from the fibrino-purulent effusion. Flow phenomena cannot be seen in cases of fibrinous and sometimes even in cases of fibrino-purulent effusion (Nuss 2003, Kofler 2009, Kofler 2011, Altenbrunner-Martinek et al. 2017).

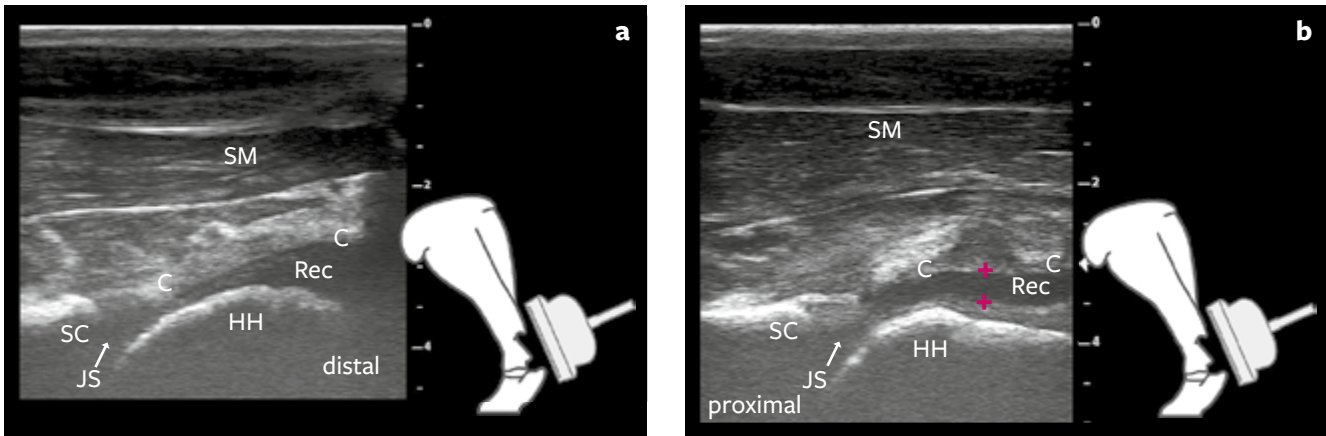


Fig. 7-5a, b: Longitudinal sonogram (10MHz linear) of the craniolateral (a) and the lateral aspect (b) of the shoulder joint in a four-week-old Simmental calf (suffering from polyarthritis) showing a septic serous arthritis. The echoic joint capsule (C) is slightly extended from the articular bone surface, showing a mild anechoic effusion of the joint pouch (Rec); smooth hyperechoic surface of the distal end of the scapula (SC), joint space (JS), smooth hyperechoic and convex surface of humeral head (HH) and the supraspinous muscle (SM). Distension of the joint pouch is indicated by the pink cursors (+) measuring a width of approximately 5 mm.

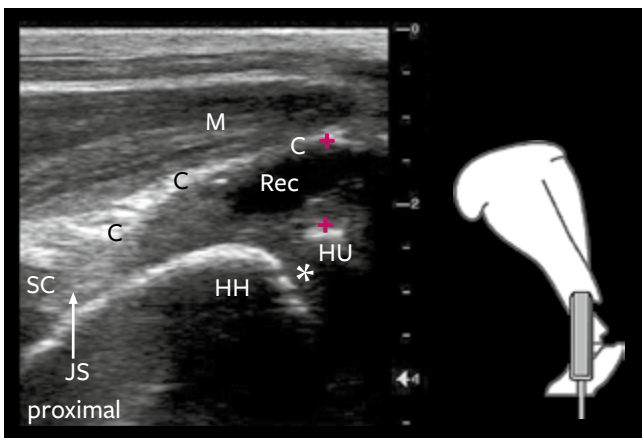


Fig. 7-6: Longitudinal sonogram (7.5 MHz linear) of the laterocaudal aspect of the shoulder joint in a four-month-old Brown-Swiss calf showing a septic serous arthritis. The echoic joint capsule (C) is markedly extended from the smooth hyperechoic and convex articular surface of the humeral head (HH), showing moderate and mainly anechoic effusion of the joint pouch (Rec). The pink cursors (+) measured a width of 10 mm; the smooth hyperechoic surface of the distal end of the scapula (SC), joint space (JS), the small anechoic interruption represents the cartilaginous growth plate (*) between the humeral head and humerus (HU); muscles (M). The caudal part of the scapulohumeral joint pouch should preferably be used for arthrocentesis because the distance from the skin to the joint pouch is lower compared to that from the lateral or the craniolateral directions.

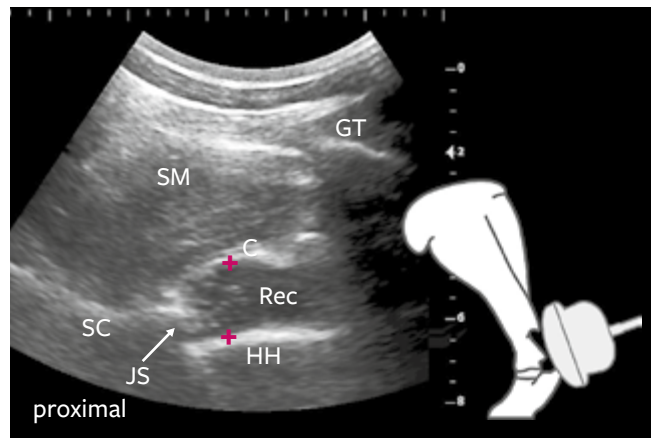


Fig. 7-7: Longitudinal sonogram (5 MHz convex) of the cranio-lateral aspect of a two-year-old Simmental heifer showing a septic serofibrinous arthritis of the scapulohumeral joint. The joint pouch (Rec) is distinctly distended (approximately 2.2 cm) as indicated by the pink cursors (+). There is a mainly anechoic effusion with some small hypoechoic spots dorsally showing flow phenomena; the pouch is surrounded by an echoic joint capsule (C); the normal hyperechoic contour of the scapula (SC) and the humeral head (HH) with the joint space (JS) in-between; the supraspinous muscle (SM); the hyperechoic contour of the greater tubercle (GT).

11.5 Normal ultrasonographic appearance of the anatomical structures

Ultrasonographically, tendons and ligaments are easily identified as linear and parallel arrangements of echoic fiber bundles in the longitudinal view, and as homogeneous echoic structures with elliptical, rounded-to-half-moon-shapes in the transverse view (Kofler and Edinger 1995, Kofler 2000, Kofler 2009, Hagag and Tawfik 2018) (► Fig. 11-1). With modern ultrasound units, a so-called **extended field of view image** can be created. Diagnostic capabilities are increased by this **panoramic view** and the images are more easily interpreted (Weng et al. 1997). The tendons in the longitudinal plane can be visualized in almost anatomical detail (► Fig. 11-2).

Since the extended field of view image makes it possible to depict an anatomic structure over its entire length, it may eliminate the need for several landmarks and multiple reference points in the near future (reference points for locating lesions accurately).

The lumina and borders of the three compartments of the common digital flexor tendon sheath at the metacarpo- and metatarsophalangeal joint regions (Stanek 1988b, Dyce et al. 2002, König and Liebich 2014, Hagag and Tawfik 2018) cannot be visualized in healthy limbs. An exception is the dorsal part of the outer proximal compartment, which appears as a narrow anechoic area (Kofler and Edinger 1995, Tryon and Clark 1999, Gonçalves et al. 2014, Hagag and Tawfik 2018). Both the longitudinal and the transverse ultrasonographic planes allow for good overviews of the entire length of the

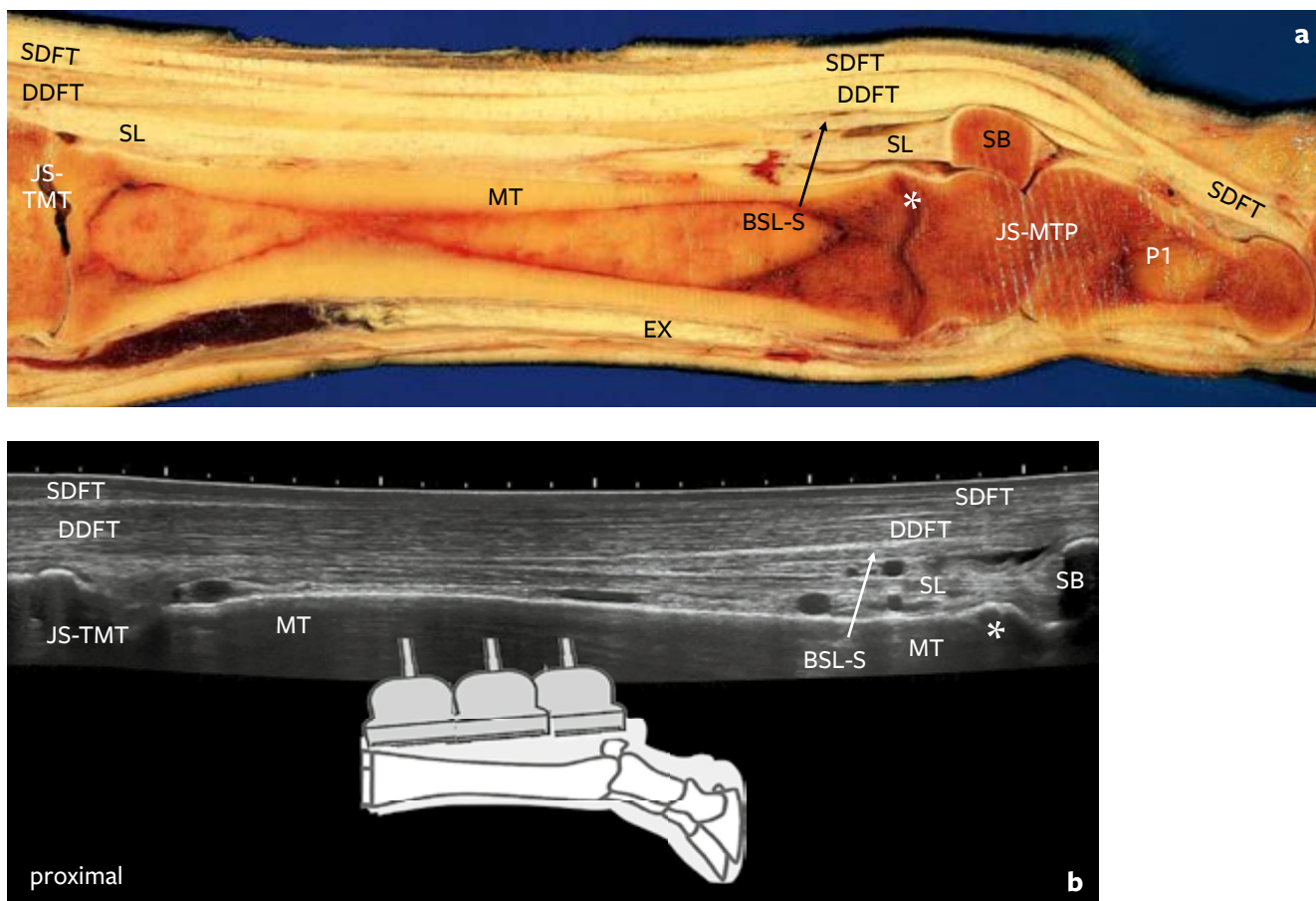


Fig. 11-1a, b: Longitudinal (sagittal) anatomical section of the metatarsus of a 14-month-old crossbreed heifer (a) and corresponding longitudinal extended field of view (length approximately 25 cm) sonogram (10 MHz linear) of the tendons at the plantar aspect of the metatarsus in a twelve-month-old Holstein heifer (b). Joint space of the tarsometatarsal joint (JS-TMT), superficial digital flexor tendon (SDFT), deep digital flexor tendon (DDFT), suspensory ligament (SL), the branch of the SL to the superficial digital flexor tendon (BSL-S), sesamoid bone (SB), contour of the metatarsal bone (MT), distal cartilaginous growth plate (*) of metatarsal bones III and IV, extensor tendon (EX), joint space of the metatarsophalangeal joint (JS-MTP), phalanx I (P1).

tendon sheath. With the transverse view, the tendon sheath of the adjoining partner digit can be directly compared and checked for differences. In addition to both common digital flexor tendon sheaths, the plantar/palmar pouch of the fetlock joint can be visualized in one single view (“**three-chamber-view**”) (Kofler and Edinger 1995, Tryon and Clark 1999, Kofler 2009) (► Chap. 4).

In healthy animals, the extensor and flexor tendons at the carpal, tarsal and fetlock joints can be recognized without difficulty by their typical texture. Again, their tendon sheaths cannot be imaged because of the small amount of synovial fluid normally present (Flury 1996, Kofler 2000, Kofler 2009, Kofler et al. 2014).

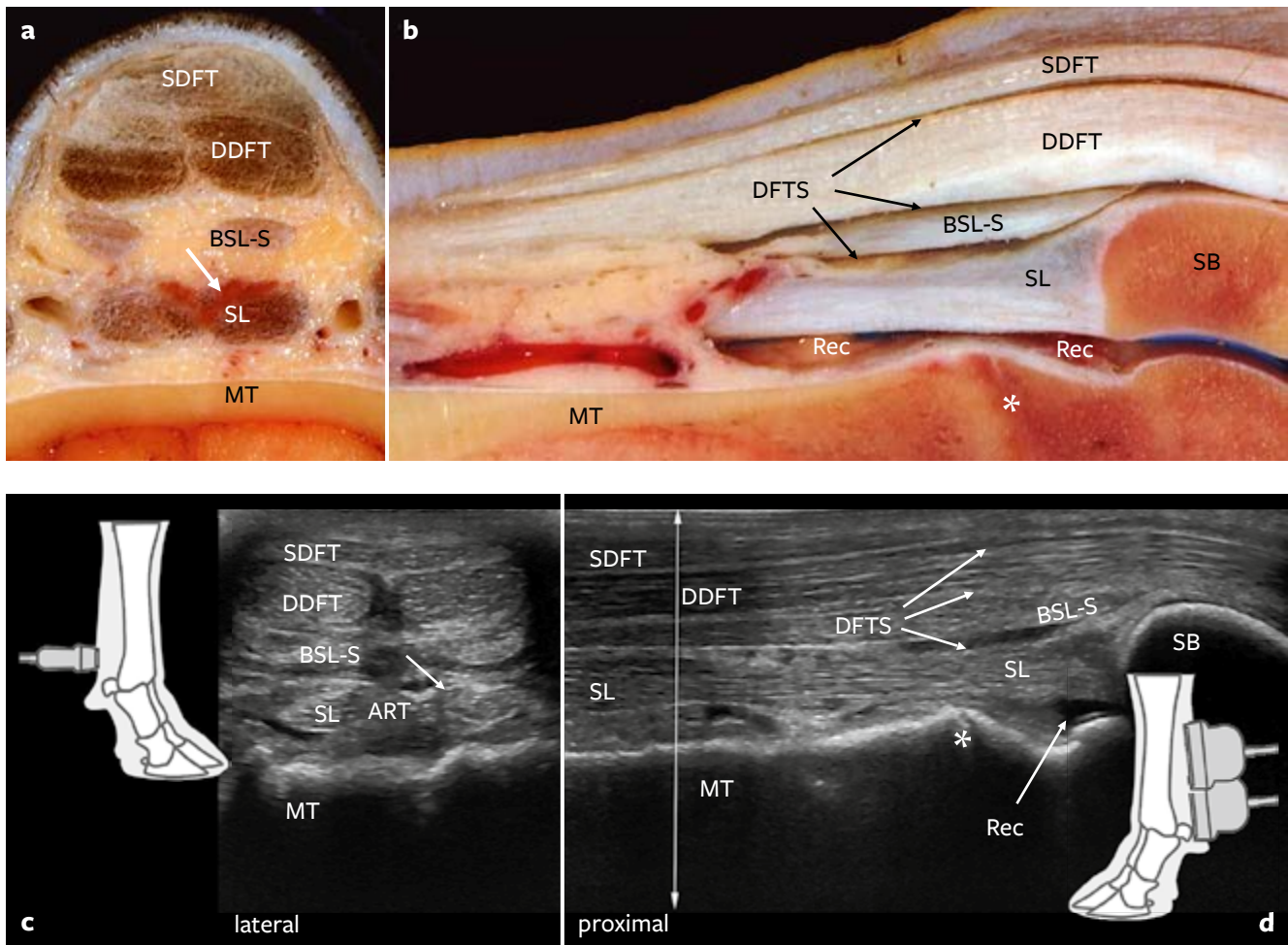


Fig. 11-2a–d: Transverse (**a**) and longitudinal (**b**) anatomical sections of the distal metatarsal region of a 16-month-old crossbreed heifer and corresponding transverse (**c**) and longitudinal extended fields of view sonograms (**d**) (10 MHz linear) of the tendons and the suspensory ligament (interosseus medius muscle). The muscular tissue (**thick white arrow**) in the interosseus medius branch to the sesamoids, visible in the anatomic section, cannot really be identified in the ultrasonographic image (► Fig. 11-2c, same region, **white arrow**). The characteristic ultrasonographic appearance of the tendons with strong linear and parallel fiber alignments can be perceived in the longitudinal plane, and a homogenous echoic texture with an elliptical, rounded or half-moon shape, depending on the tendon/ligament, in the transverse plane. The probe was positioned exactly perpendicular to the tendon/ligament.

Superficial digital flexor tendon (**SDFT**), deep digital flexor tendon (**DDFT**), branch of the SL to the superficial digital flexor tendon (**BSL-S**), the normal small lumen (**DFTS**) of the digital flexor tendon sheath and the suspensory ligament branches (**SL**). A characteristic edge-shadowing artifact (**ART**) occurs between the axial edges of the flexor tendons in the transverse plane. It obstructs the view to the interdigital branch of the suspensory ligament. The smooth hyperechoic contour of the metatarsal (**MT**) and sesamoid bones (**SB**), and the distal cartilaginous growth plate (*****) of the fused 3rd and 4th metatarsal bones are landmarks to localize the normal plantar recess (**Rec**) of the fetlock joint. The **transverse double arrow** positioned in the longitudinal ultrasonographic view indicates the level where the transverse view was obtained.

11.6 Sonopathological findings

11.6.1 Tear or rupture of tendons/ligaments

In contrast to the horse, traumatic lesions of tendons and ligaments are less frequently encountered in cattle (Anderson and St-Jean 1996, Dirksen 2006, Anderson et al. 2008, Steiner et al. 2014, Nuss et al. 2017a). A traumatic lesion (tear or rupture) caused by closed internal trauma results in obvious changes in the texture and echogenicity of the affected tendons (►Fig. 11-3). These lesions are imaged as hypo- or anechoic areas within the tendon or ligament

fiber bundles, most likely caused by stretched or torn fibers, and are associated with fluid accumulation and hematoma formation (Boppart 2013, Nuss et al. 2017a). The normal parallel fiber alignment is lost, the cross section diameter of the tendon/ligament is enlarged, and the tendon or ligament fibers show a tortuous appearance.

With incomplete or complete rupture, the stump of the tendon can be identified at some distance proximal to the wound or the level of rupture (►Fig. 11-4) due to muscle contraction. Debris and/or air are usually imaged, as well as fluid accumulation (Boppart 2013, Nuss et al. 2017a).

Once a tendon sheath is affected by aseptic inflammation, anechoic or increasingly echoic effusion can be imaged

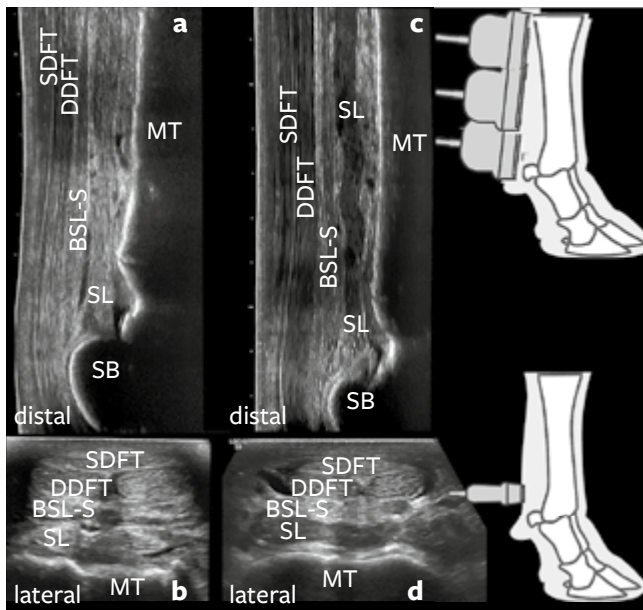


Fig. 11-3a-d: Longitudinal extended field of view (a) and transverse sonogram (b) (10 MHz linear) of the plantar aspect of the metacarpal region of a healthy heifer. Longitudinal extended field of view (c) and transverse wide view sonogram (d) (10 MHz linear) of a twelve-month-old heifer with rupture of the suspensory ligament. The hypoechoic-to-anechoic density and the tortuous texture of the suspensory ligament branches (SL) running to the sesamoid bones (SB) indicate torn fibers and fluid accumulation in the SL due to the rupture. The superficial digital flexor tendon (SDFT), the deep digital flexor tendon (DDFT), the branch of the SL to the superficial digital flexor tendon (BSL-S), and the smooth and hyperechoic contours of the metatarsal bone (MT).

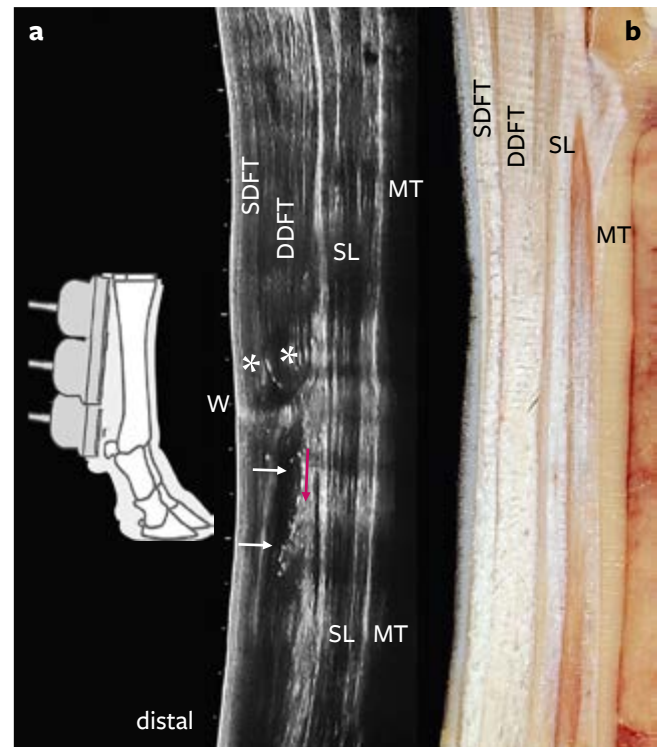


Fig. 11-4a, b: Longitudinal extended field of view sonogram (10 MHz linear) (a) of a five-year-old Brown Swiss cow showing complete rupture of the superficial (SDFT) and deep digital flexor tendons (DDFT) at approximately the mid-level of the metatarsal bone (MT). This severe tendon injury was associated with an open wound (W) following sharp trauma. The proximal stumps (*) of the DDFT and SDFT are depicted in the center of the image. Bright spots distal to the stump indicate gas and debris accumulation in the soft tissue (white arrows). Only a few tendon fiber residues (pink arrow) can be identified in this area. The suspensory ligament (SL) appears normal. The corresponding anatomical section (b) shows the relevant anatomical structures.

around the tendon(s) and up to the musculotendinous junction (► Fig. 11-5). For example, inflammation of the carpal extensor tendons and its sheaths is characterized by swelling of the tendon and the presence of hypoechoic and/or echoic effusion indicating fibrin clots and granulation tissue (► Fig. 11-5a). This latter condition is very painful and carries a poor prognosis (Klee and Hänichen 1989).

Similar ultrasonographic findings can be depicted when the lateral collateral ligament and the tendons of insertion and origin of the muscles at the lateral stifle joint region are affected. This periarticular inflammation of the lateral stifle joint region is a disorder commonly observed in cows that have difficulty with rising around parturition time in particu-

lar in a tied stall environment. A subacute pressure-induced inflammatory process is initiated, which leads to alteration of the muscle origins, the lateral collateral ligament and the bursa of the gluteobiceps tendon at the stifle (Nuss et al. 2011a). Ultrasonographically, echoic material around the tendons, fluid accumulation in the swollen musculotendinous junction, loss of the typical texture of the involved tissues, signs of tissue necrosis and other changes in close vicinity to the tendon origins and the lateral collateral ligament of the stifle can be imaged (► Fig. 11-5b).

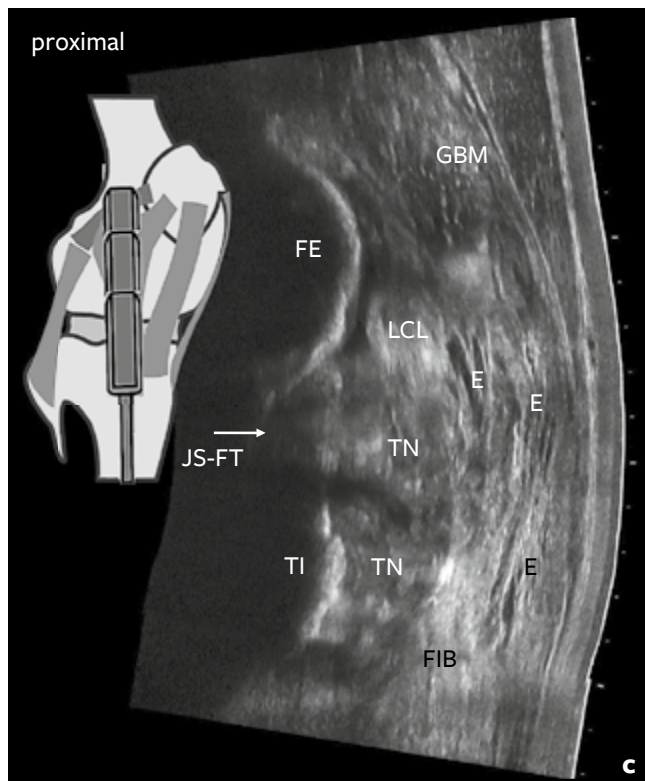
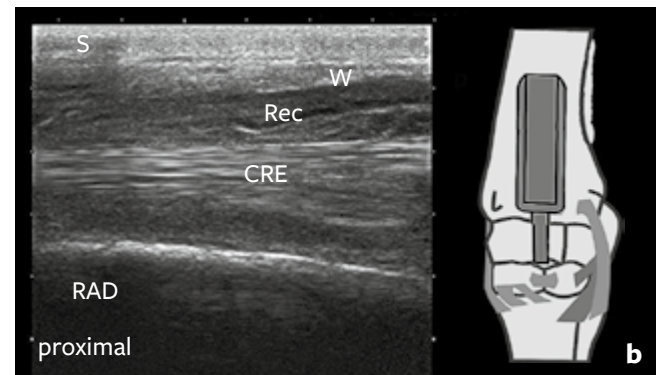
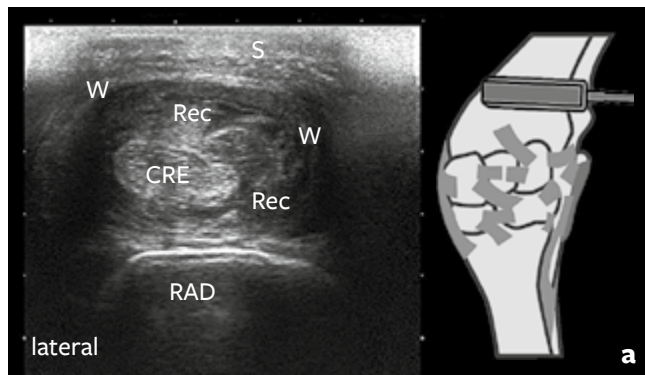


Fig. 11-5a–c: Transverse (a) and longitudinal sonograms (b) (10 MHz linear) of the cranial aspect of the distal forearm of a five-year-old Brown Swiss cow showing aseptic granulomatous inflammation of the carpal radial extensor tendon (CRE) and its tendon sheath (bursa) at the musculotendinous transition and distally; this synovial cavity (Rec) is distinctly distended and filled with an echoic content indicating granulomatous inflammation; the contour of the radius (RAD), the tendon sheath wall (W), skin and subcutaneous tissue (S).

Longitudinal extended field of view sonogram (10 MHz linear) (c) of the lateral aspect of the right stifle region of a 28-month-old cow showing an aseptic (chronic pressure-induced) inflammatory process of the tendons, muscles and the bicipital femoral bursa in the lateral stifle region. Edema and swelling of the subcutaneous tissue (E), showing the characteristic honey-comb-like texture (small anechoic areas surrounded by thin echoic connective tissue strains) are visible. Parts of the adjoining muscles, parts of the lateral collateral ligament (LCL) and the tendon of origin of the long fibular muscle (FIB) are not well differentiated due to swelling and loss of normal texture. Anechoic fluid accumulation at the musculotendinous junction indicates tissue necrosis (TN) caused by chronic ischemia. The lateral condyle of the tibia (TI), the femoral bone (FE), femorotibial joint space (JS-FT, arrow), and the gluteobiceps muscle (GBM).



Fig. 18-5a, b: Lateral view of an eight-week-old Simmental calf showing the position of the 7.5 MHz linear probe for ultrasonographic examination of the spinal cord at the atlanto-occipital window in longitudinal (**a**) and transverse planes (**b**) in the standing animal. The head of the calf is held in a strongly flexed position.



Fig. 18-6a, b: Lateral view of an eight-week-old Simmental calf showing the position of the 7.5 MHz linear probe for ultrasonographic examination of the spinal cord at the lumbo-sacral window between the 6th lumbar and 1st sacral vertebrae in longitudinal (**a**) and transverse planes (**b**) in the standing animal.

18.5 Normal ultrasonographic appearance of the spinal cord in the three acoustic windows

18.5.1 Atlanto-occipital acoustic window

The atlanto-occipital acoustic window corresponds to the junction between the occiput and the atlas. In the sagittal plane, the spinal cord appears as a homogeneous tubular hypoechoic structure that is curved cranio-ventrally, with echoic margins referable to the pia mater and a well-defined echoic central line corresponding to the central canal (► Fig. 18-7a).

The subarachnoid space appears as an anechoic area dorsal and ventral to the spinal cord due to the normal presence of cerebrospinal fluid. The subarachnoid space is externally delimited by a hyperechoic line referable to the dura mater together with the arachnoid and coinciding with the margin of the spinal canal. In fact, the dura mater and arachnoid membrane cannot be differentiated from each other ultrasonographically.

Cranially the spinal cord shows an enlargement corresponding to its transition into the medulla oblongata at the level of the great foramen, whereas the central canal is displaced dorsally. At this point it is possible to image ultrasonographically an anechoic triangular space, whose size may vary depending on the degree of head flexion: it corresponds to the caudal portion of the cerebrospinal fluid-filled fourth cerebral ventricle. By flexing the head, it is possible to highlight additionally echoic structures consistent with parts of the medulla oblongata, pons and cerebellum (► Fig. 18-7a). In the transverse view, the spinal cord appears as an ellipsoid hypoechoic structure with echoic margins (pia mater). The central canal is visible as an echoic dot that is surrounded by a hypoechoic butterfly-shaped image in the transverse plane, corresponding to the grey matter. In the transverse plane, the subarachnoid space has a mildly echoic, striated appearance that may not be so evident in sagittal imaging. This echoic lattice is due to the presence of the trabeculae of the subarachnoid space that connect the arachnoid and pia mater.

If the probe is angled at 45° cranio-ventrally, the caudal portion of the fourth cerebral ventricle appears as an anechoic semilunar space between the spinal cord and the subarachnoid space.

Lateral to the spinal cord, it is possible to image the emergence of the echoic denticulate ligaments as well as

the emergence of the echoic dorsal and ventral roots, respectively, dorsal and ventral to the denticulate ligament. Round anechoic areas can be depicted dorsolateral to the echoic dura mater: they can be confirmed by color Doppler examination to be vessels in the hypoechoic epidural space. The presence of fat and/or connective tissue in the epidural space explains its slight echogenicity. Dorsal to the neural structures it is possible to differentiate the dorsal atlanto-occipital membrane (a thick hyperechoic band) and the major dorsal straight muscle of the head.

Laterally, the rims of the occipital condyles are represented by two hyperechoic medially concave curved lines, which are responsible for distal acoustic shadowing (► Fig. 18-7b) (Testoni et al. 2010a, b, Testoni et al. 2012, Gentile et al. 2012, Braun et al. 2015, Braun and Attiger 2016).

18.5.2 Lumbar acoustic window

The lumbar acoustic window corresponds to the L5-L6 interlumbar space. In the sagittal plane, the spinal cord appears as a hypoechoic tubular structure with echoic margins (pia mater) and a central echoic single line corresponding to the central canal. The spinal cord is surrounded by the anechoic cerebrospinal fluid in the subarachnoid space. The arachnoid-dura mater complex corresponds to the echoic margin of the spinal canal dorsal and ventral of the subarachnoid space (► Fig. 18-8a). The epidural space can be imaged as a thin hypoechoic space adjacent to the arachnoid-dura mater complex (hyperechoic line).

A transverse view of the spinal cord shows the hypoechoic, oval spinal cord with the echoic central echo and the echoic pia mater directly surrounding the spinal cord lying within the anechoic subarachnoid space (► Fig. 18-8b). It is not always possible to differentiate the butterfly-shaped grey matter of the spinal cord in the interlumbar window. The spinal cord gives rise to the paired echoic dorsal and ventral nerve roots, and it is fixed in position by the denticulate ligaments, which merge laterally from the spinal cord as echoic structures.

The surfaces of the vertebral bodies appear as hyperechoic contours ventral to the spinal cord. The hyperechoic vertebral arches produce ventral acoustic shadows on transverse views, and the hyperechoic contours of the spinous processes dorsally produce ventral acoustic shadows in sagittal views. The epaxial muscles appear as hypoechoic areas adjacent to the laminae (► Fig. 18-8b) (Testoni et al. 2010a, b, Testoni et al. 2012, Gentile et al. 2012, Braun and Attiger 2016).

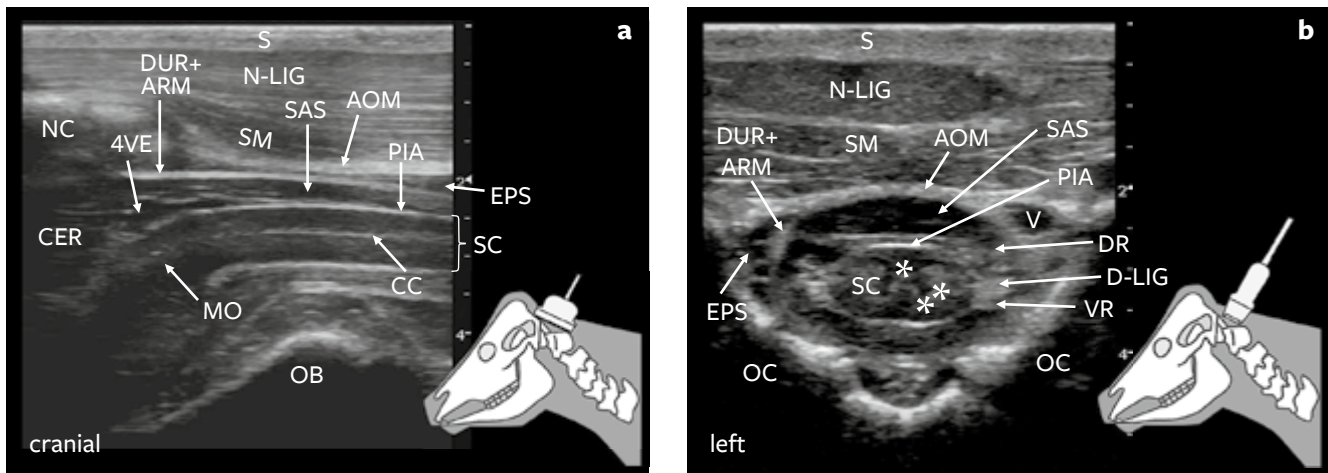


Fig. 18-7a, b: Sagittal (a) and transverse (b) sonograms (7.5 MHz linear) of the spinal cord taken at the atlanto-occipital acoustic window of a one-month-old Holstein calf, showing a normal ultrasonographic appearance of the relevant anatomical structures; in order from outside to inside: the skin (S), the nuchal ligament (N-LIG), the nuchal crest (NC) of the occipital bone, the major dorsal straight muscle of the head (SM), the thick echoic dorsal atlanto-occipital membrane (AOM), the anechoic epidural space (EPS), the echoic dura mater with the arachnoid membrane (DUR+ARM), the anechoic subarachnoid space (SAS), the echoic pia mater (PIA), the homogeneous tubular hypoechoic spinal cord (SC) with the thin echoic central canal (CC) originating cranially from the medulla oblongata (MO); the cerebellum (CER), the anechoic 4th ventricle (4VE), the hyperechoic contour of the occipital bone (OB). All of these structures can also be differentiated in the transverse sonogram (b). Furthermore, the gray (*) and white matter (**) of the spinal cord (SC), the dorsal (DR) and ventral roots (VR) of the segmental nerves and the denticulate ligament (D-LIG) can be distinguished; vessel (V) and the hyperechoic contour of the occipital condyles (OC).

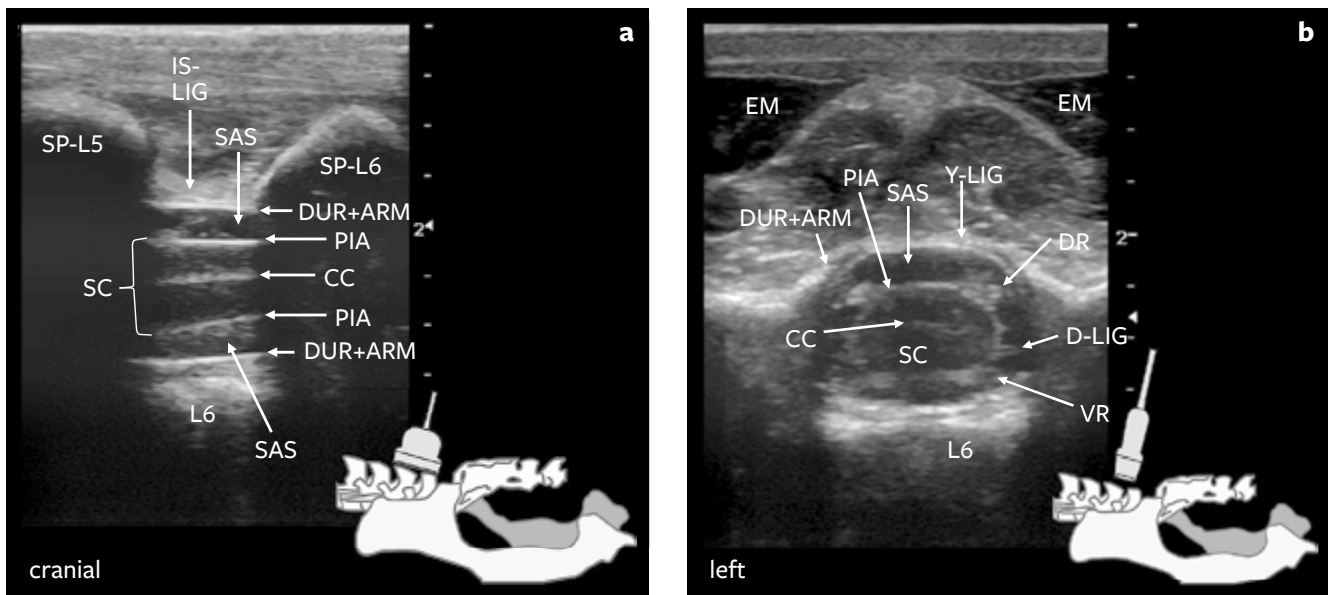


Fig. 18-8a, b: Sagittal (a) and transverse (b) sonograms (7.5 MHz linear) of the spinal cord taken at the lumbar window between the spinous processes of the 5th (SP-L5) and 6th lumbar vertebrae (SP-L6) of a one-month-old Holstein calf showing a normal ultrasonographic appearance of the relevant anatomical structures: the echoic interspinous ligament (IS-LIG), the echoic dura mater with the arachnoid membrane (DUR+ARM), the anechoic subarachnoid space (SAS), the echoic pia mater (PIA), the homogeneous tubular hypoechoic spinal cord (SC, bracket) with the thin echoic central canal (CC); and the hyperechoic contour of the vertebral body of L6. All these structures can also be differentiated in the transverse sonogram (b). Further, the echoic dorsal (DR) and ventral roots (VR) of the segmental nerves, the echoic denticulate ligament (D-LIG) and the yellow ligament (Y-LIG) dorsally are visible. The epaxial muscles (EM) appear as hypoechoic areas located dorsal to the vertebral arch.

Index

- A**
- Abdominal aorta 122, 124, 126, 160, 163, 167
 - thrombosis 135
 - Abscess 11, 12, 22
 - carpal region 55, 63, 64
 - coxofemoral region 135
 - differentiation 22
 - elbow region 67
 - fetlock joint region 47
 - gluteal muscles 135
 - intramuscular 152
 - intramuscular injection 135
 - pelvic region 135
 - periarticular 18, 35
 - peritarsal 100
 - shoulder joint region 88
 - spinal cord 222
 - stifle joint region 120
 - tarsal joint region 89, 94
 - Type-1/Type-2 22
 - ultrasound-guided puncture 236
 - Accessory carpal bone 17
 - Acetabular fossa 122
 - Acetabular lip 122, 126, 127
 - Acetabular rim 125
 - Acetabulum 122, 124, 126
 - Acoustic enhancement, distal 6, 7
 - Acoustic shadowing, distal 7
 - Acoustic waves 3
 - Acoustic window 221
 - atlanto-occipital 221, 222, 223, 226, 227, 229, 231
 - interlumbar 222, 223, 226, 228
 - lumbar 223, 226, 229, 230
 - lumbosacral 223, 228
 - Anatomical landmarks 12
 - antebrachiocondylar joint 52
 - backfat 206, 207
 - brachial plexus 214, 216
 - carpometacarpal joint 52
 - coxofemoral joint 124
 - distal interphalangeal joint 26
 - distal intertarsal joint 93
 - elbow joint 68
 - femoral nerve 216
 - fetlock joint 37
 - metacarpophalangeal joint 37
 - metatarsophalangeal joint 37
 - middle carpal joint 52
 - peripheral nerves 214
 - proximal interphalangeal joint 26
 - sciatic nerve 214, 216
 - shoulder joint 81
 - spinal cord 223
 - stifle joint 107, 108
 - tarsal joint 93
 - tarsocrural joint 93
 - tarsometatarsal joint 93
 - tendons 138
 - tendon sheaths 139
 - Anesthetic blocks 211
 - Arachnoid (arachnoid membrane) 222
 - Arnold-Chiari-like malformation 229
 - Arteries
 - anatomy 160
 - brachial artery 167
 - common carotid artery 159
 - cranial femoral artery 214
 - cranial tibial artery 90, 160
 - dorsal common digital artery III 37, 38, 160, 161, 162, 167, 169, 174
 - dorsal metatarsal artery III 160, 161, 167, 174
 - dorsal pedal artery 15, 160, 166
 - external iliac artery 122, 126, 163, 167
 - interdigital artery 160, 161, 174
 - internal iliac artery 122, 163
 - lateral palmar/plantar digital artery 38, 39
 - lateral saphenous artery 90, 160
 - mean lumen diameters 167
 - medial palmar/plantar digital artery 38, 39
 - medial saphenous artery 160
 - median artery 160, 164, 167
 - median sacral artery 122
 - normal ultrasonographic appearance 164
 - palmar common digital artery 37
 - palmar common digital lateral/medial artery 160
 - plantar common digital artery IV 162, 169
 - plantar common digital lateral/medial artery 160
 - popliteal artery 106, 109, 110, 167
 - radial artery 160, 164, 167
 - uterine artery 159
 - Arthritis
 - carpal joint 51, 55, 63
 - coxofemoral 128
 - distal interphalangeal joint 29, 35, 144, 168, 169
 - elbow joint 67, 69, 72
 - fetlock joint 35, 42, 45, 144
 - metacarpophalangeal joint 35, 40
 - metatarsophalangeal joint 40
 - proximal interphalangeal joint 25, 30, 35, 144
 - proximal intertarsal joint 98, 100
 - scapulohumeral joint 79, 84, 85
 - septic 11, 12
 - shoulder joint 79, 85, 87
 - stifle joint 105, 112
 - tarsal joint 89, 96
 - tarsocrural joint 96, 97, 98, 100
 - traumatic 12, 18
 - ultrasound-guided intervention 238
 - Arthrocentesis 25, 31
 - coxofemoral joint 129
 - pneumarthrosis 25
 - ultrasound-guided 234
 - Arthrosis
 - interphalangeal joint 25
 - Articular cartilage 13, 38, 69, 70, 81, 109, 125, 134, 176, 189
 - Artifacts 4
 - acoustic enhancement 6, 14, 29, 162
 - acoustic shadowing 7
 - comet-tail 5
 - double image 5
 - edge-shadowing 8, 43, 138, 141
 - electrically induced 8
 - fan 8

Index

- refraction 5
- reverberation 5, 14, 22
- ring-down 5, 22, 32, 112, 156
- slice thickness 5
- Atlanto-occipital membrane 223, 226
- Atlanto-occipital region 222
- Atlanto-occipital space 222
- Attenuation 3
- Avulsion fracture
 - origin of the common digital extensor muscle 75
- Axial resolution 4

B

- Backfat
 - measurement 205, 206
 - reference values for different breeds 208
 - thickness 205, 208
- Blood flow
 - profiles 174
- Blood vessels 13
- B-mode ultrasonography 159
- Body condition score (BCS) 200, 208
- Bone 175
 - anatomy 175
 - infections 183
 - lysis 183
 - sequestrum 187
 - subchondral cysts 189
 - tumors 192
- Bone fissure 177
- Brachial plexus 214
 - anatomy 213
 - block 213
- Bursa 12
 - bicipital 19, 79, 82
 - femoral bicipital 105, 106, 119, 149
 - infraspinous 79, 82
 - of the gluteobiceps tendon 137
 - of triceps brachii muscle 70
 - podotrochlear 26, 28, 138, 194
 - subcutaneous of olecranal tuberosity 68, 70
 - subtendinous calcaneal 21, 90, 95, 100, 102, 137, 186
 - subtendinous of the biceps femoris muscle 119
 - subtendinous of the triceps brachii muscle 68, 70
- Bursitis 11, 12
 - bicipital bursa 79, 86
 - femoral bicipital bursa 105
 - infraspinous bursa 79, 86
 - lateral tarsal 19, 94, 97, 100, 101

- precarpal 17, 19, 20, 51, 54, 55, 60, 62
- stifle joint 119
- subcutaneous calcaneal 21, 97, 100
- subtendinous calcaneal 19, 89, 97
- tarsal 21, 168

C

- Calcaneal tuber 21, 90, 91, 92, 93, 94, 100, 176, 186
- Calcinosis 160, 172
 - abdominal aorta 172
- Capital femoral physis 126
- Carpal bone
 - accessory 17
 - intermediate 19, 20
- Carpal region 51, 53
- Carpal tunnel syndrome 137
- Carpus 52
- Caudal branch of the lateral saphenous vein 8, 14, 15, 103, 160, 166, 167, 168
- Centesis
 - atlanto-occipital 221
 - coxofemoral joint 129
 - pneumarthrosis 25
 - ultrasound-guided 234
- Central canal 223, 224, 226, 229
- Cerebrospinal fluid 226, 228
 - collection, ultrasound-guided 234
- Chondrosarcoma 192
- Claw horn 193
 - moisture content 195
 - thickness 195
- Congenital malformations of spinal cord 229
- Connective tissue 13
- Continuous wave (CW) Doppler 159
- Contusion, muscles 147
- Core lesions 145
 - infected digital flexor tendons 144
- Coxal tuber 124, 126, 127, 206, 207
- Cranial branch of the lateral saphenous vein 15, 103, 160, 166, 167, 168
- Cysts, spinal cord, fluid-filled 229

D

- Degenerative joint disease (DJD) 134
 - coxofemoral joint 134
 - femorotibial joint 134
 - scapulohumeral joint 134
 - tibiotarsal joint 134
- Diffuse reflection (scattering) 3
- Digital fat cushion 197
 - thickness 193, 200

- Diplomyelia 229
- Dislocation, humeral head 87
- Disruption
 - gluteobiceps muscle 152
- Doppler ultrasound 159
 - color Doppler 159, 226
- Dura mater 222

E

- Echogenic needle 211, 212, 214, 235, 238
- Edema 35, 47, 54, 64, 94, 99, 100, 120
 - subcutaneous inflammatory 16, 18, 19, 23
- Effusion, echogenicity 12
- Elbow joint 67
- Elevational resolution 3
- Enthesiophytes 99
- Epidural space 222, 226
- Epineurium 216
- Exostosis
 - distal phalanx 201
- Extensor retinaculum
 - distal 91
 - proximal 91, 95, 96

F

- Fascia
 - lata 149
 - of gluteal muscle
 - deep 206, 207
 - intramuscular 207
 - superficial 206, 207
- Fat pad, infrapatellar 106, 107, 109
- Fat tissue 13
- Femoral head 126
- Femoral neck 126
- Femoral nerve block 213
- Fibrosarcoma 192
- Fine-needle aspiration biopsy, ultrasound-guided 234
- Fissure 177
- Flexor tubercle 196, 197, 200
- Flow phenomena 12, 14, 16, 18, 21, 22, 23, 32, 101, 233
- Focal zone 4
- Forelimb anesthesia, brachial plexus block 213
- Fracture 175, 177
 - acetabulum 121
 - carpal intra-articular 51
 - diaphyseal 180
 - distal phalanx 193

- femoral 105
 - femoral capital physeal 121, 132
 - femoral neck 132
 - greater tubercle of humerus 87
 - hematoma 177, 178
 - humerus 67, 75
 - ilial shaft 180
 - metacarpal 48, 178
 - metatarsal 48, 179, 180
 - olecranon 75
 - pedal bone 177, 203
 - pelvic bones 124, 132, 177
 - phalanges 25, 33
 - proximal radius 75
 - rib 129
 - sacral vertebrae 181
 - scapula 79
 - scapular spine 87
 - shoulder joint 87
 - tibia 105
 - ultrasonographical characterization 132
- Free-hand ultrasound-guided centesis 234

G

- Glenoid cavity 79
- Glenoid tubercle 80
- Greater trochanter 122, 126, 127, 176, 213
- Greater tubercle 81, 82, 87, 176
- Growth plate 13, 176
 - apophysis of the greater trochanter 127
 - calcaneal tuber 93
 - distal femur 106, 108, 109, 113, 117
 - distal humerus 69
 - distal tibia 93, 94
 - femoral bone 122
 - femoral head 122, 127, 132
 - femoral neck 122, 132
 - greater tubercle 80
 - humeral head 85
 - humerus 68, 69, 82, 85
 - lateral malleolus 93
 - metacarpus/metatarsus 38
 - metatarsal bones 140
 - olecranal tuberosity 68
 - proximal radius 68, 69
 - proximal tibia 106, 108, 109, 111
 - supraglenoid tubercle 81, 82
 - tibial tuberosity 108, 109, 110
 - ulna 69

H

- Hemarthrosis
 - coxofemoral joint 132
 - stifle joint 118
- Hematoma 11, 12, 18, 22
 - differentiation 22
 - fetlock joint 47
 - fracture 177, 178
 - gluteal muscles 135
 - muscles 152
 - pelvic region 135
- Herniation
 - synovial 22
- Hindlimb anesthesia, sciatic and femoral nerve block 213
- Humerus 82
- Hydromyelia 221, 229
- Hydrops
 - tendon sheath 144
- Hydro-syngomyelia 229
- Hygroma
 - carpal 17
 - lateral tarsal 19, 89, 94, 97, 100, 101
 - precarpal 19, 20, 54, 62
- Hyperechoic reflections/spots (snow-flurry-like) 20, 22
- Hyperemia
 - metacarpal arteries 168
 - metatarsal arteries 168
- Hypoplasia, spinal cord 229

I

- Inflammation
 - carpal radial extensor tendon 143
 - common digital flexor tendon sheath 145
 - deep digital flexor tendon 144, 146
 - lateral stifle joint 143
 - muscle 152
 - of the carpal extensors 138
- Interlumbar space 222
- Intramuscular injection, inappropriate 219
- Intravascular injections, inadvertent 211
- Intravenous regional limb perfusion 159
- Ischial tuber 122, 123, 206, 207

J

- Joint capsule 13, 16
- Joint recess 13
- Joint/s 12
 - antebrachioacarpal joint 17, 19, 51, 52
 - atlanto-occipital 222
 - carpal joint 17, 20, 51, 52, 138
 - carpometacarpal joint 20, 51, 52

- coxofemoral joint 121, 122, 124, 127, 213, 236, 238
 - distal interphalangeal joint 25, 26, 27, 138, 194
 - distal intertarsal joint 90, 93
 - elbow joint 67
 - femoropatellar joint 106, 108, 109, 110
 - femorotibial joint 106, 107, 108, 109
 - fetlock joint 8, 18, 19, 35, 137
 - hip joint 122
 - lumbosacral joint 2
 - metacarpophalangeal joint 16, 35, 67, 89, 140
 - metatarsophalangeal joint 18, 35, 140
 - middle carpal joint 20, 51, 52, 138
 - pastern joint 137
 - proximal interphalangeal joint 25, 26, 27, 30
 - proximal intertarsal joint 16, 89, 93
 - sacroiliac joint 122, 123, 124, 126
 - scapulohumeral joint 81, 82, 84, 237
 - shoulder joint 19, 79
 - stifle joint 105, 107
 - suprapatellar joint 108
 - tarsal joint 89
 - tarsocrural joint 14, 15, 20, 67, 89, 90, 93, 237
 - tarsometatarsal joint 90, 93
 - ultrasound-guided interventions 233
- Joint space 13, 16

L

- Laceration
 - muscles 147
- Laminitis, chronic 194, 200, 201
- Lateral resolution 4
- Ligament/s 13
 - accessoriometacarpal 17
 - caudal cruciate 106
 - collateral 12, 48
 - of carpal joint 51
 - of stifle joint 118
 - cranial cruciate 106
 - cruciate 12, 105, 106, 109, 118
 - denticulate ligament 226, 227
 - injuries 11
 - intermediate patellar 106, 108, 109, 110, 112, 113
 - interspinous ligament 222, 223, 227
 - lateral collateral 35, 39
 - of stifle joint 106, 143
 - of tarsal joint 90, 94
 - lateral collateral of elbow joint 67, 70
 - lateral patellar 106, 107, 108, 109
 - long plantar 90, 91, 94, 102

Index

- medial collateral 35, 38, 39
- of stifle joint 106, 107, 112, 118
- of tarsal joint 90, 94
- medial collateral of elbow joint 67, 70
- medial patellar 106, 108, 109
- nuchal ligament 222, 227
- sacrotuberal 149
- suspensory siehe suspensory ligament 16
- yellow ligament 227
- Lumbosacral plexus 213
- Lumbosacral space 223
- Lumbosacral transition 125
- Luxation 18, 175
 - coxofemoral 121, 122, 125, 131, 182, 183
 - elbow joint 182
 - femoral head 131
 - fetlock joint 35, 48, 182
 - patellar 105
 - scapulohumeral 79
 - scapulohumeral joint 182
 - shoulder joint 87
- Lymph node, popliteal 110

M

- Manica flexoria 138
- Mechanical ultrasound-guided system 234
- Meninges 222, 231
- Meniscus 13, 106
 - injuries 118
 - lateral 110
 - medial 112
- Mesotendineum, thickened 20
- Mesotenon, thickened 146
- Metacarpal bone 16
- Metacarpal epiphysis, displaced bone 48
- Metacarpal fracture 48
- Metacarpus/Metatarsus 38
- Metatarsal epiphysis, displaced bone 48
- Metatarsal fracture 48
- Muscle injuries 147
- Muscle/s 13, 147
 - abductor pollicis longus muscle 138
 - abscess 152
 - anatomy 148
 - biceps brachii muscle 68, 71, 79, 80, 82, 137, 147, 148, 149
 - biceps femoris muscle 19, 106, 107, 108, 119
 - brachiocephalicus muscle 79, 82
 - carpal extensor muscle 138
 - carpal flexor muscle 18
 - carpal radial extensor muscle 18, 68, 71, 147, 149

- carpal ulnar extensor muscle 70
- caudal tibial muscle 92
- cleido-occipitalis muscle 24
- common digital extensor muscle 68
- cranial tibial muscle 92, 107, 111
- deltoid muscle 80, 83
- digital flexor muscle 103
- epaxial muscles 226
- gastrocnemius muscle 91, 92, 106, 137, 148, 149
- gluteal muscles 129, 131
- gluteobiceps muscle 106, 110, 147, 149, 156
- gluteus medius muscle 157
- infraspinous muscle 19, 83
- interosseus medius muscle 138, 139, 141
- lateral digital extensor muscle 18, 91, 150
- lateral digital flexor muscle 18, 91
- long digital extensor muscle 91, 150
- long fibular muscle 91, 143
- longissimus muscle 206
- medial digital flexor muscle 18
- middle gluteal muscle 206, 207
- oblique carpal extensor muscle 138
- omotransverse muscle 24, 79, 82
- popliteus muscle 106
- psoas major muscle 214
- quadriceps muscle 106, 156, 213, 214
- rectus capitis dorsalis major muscle 222
- rupture 152
- semimembranosus muscle 106, 147
- semitendinosus muscle 106, 147
- short digital extensor muscle 91
- soleus muscle 149
- subscapularis muscle 79
- superficial digital flexor muscle 90, 91, 149
- supraspinous muscle 79, 82, 83
- tears 152
- tensor fasciae latae muscle 157
- third fibular muscle 91, 92, 105, 107, 109, 111, 137, 148, 150
- trapezius muscle 79
- triceps brachii muscle 68, 71
- Musculoskeletal structures
 - impedance 3
 - ultrasonographic evaluation 1
- Musculoskeletal system, anatomical structures 13
- Musculotendinous junction 147
- Myelocoele 221
- Myelography 221
- Myelomeningocele 221
- Myosarcoma 24

N

- Necrosis
 - muscle 152
 - Nerve blocks
 - ultrasound-guided 213, 234
 - Nerve conduction block 211
 - Nerve injuries
 - sciatic nerve 135
 - Nerve/s 13, 211
 - femoral nerve 214, 216, 219
 - fibular nerve 150
 - peroneal nerve 106, 107, 109, 135, 213
 - popliteal nerve 107
 - saphenous nerve 214
 - sciatic nerve 122, 135, 213, 214, 217
 - tibial nerve 109, 213
 - Neuroparenchyma, paracentral cavitation 229
 - Neuropathies 219
- ## O
- Olecranal tuberosity 68, 69, 70, 176
 - Orientation 9
 - Osteitis 175, 183
 - carpal joint 61
 - distal growth plates of radius and ulna 51
 - distal metacarpal/metatarsal growth plate 45
 - elbow joint 75
 - fetlock joint 35
 - metacarpophalangeal joint 35
 - metatarsophalangeal joint 35
 - phalanges 25, 33
 - proximal growth plate of the proximal phalanx 45
 - shoulder joint 87
 - stifle joint 116
 - Osteoarthritis 175
 - coxofemoral joint 134
 - stifle joint 105
 - tarsal joint 89
 - Osteoarthrosis 189
 - tarsal 95
 - Osteochondrosis 175, 189
 - stifle joint 116
 - Osteolysis 185
 - acetabular rim 129
 - calcaneal tuber 103
 - distal interphalangeal joint 31
 - Osteomyelitis 175, 183
 - carpal bones 51, 61
 - distal metacarpal/metatarsal growth plate 45
 - fetlock joint 35

- growth plate of the distal humerus 75
 - inflammatory subperiosteal exudate 184
 - metacarpophalangeal joint 35
 - metatarsophalangeal joint 35
 - phalanges 33
 - proximal growth plate of the proximal phalanx 45
 - sesamoid bone 144
 - shoulder joint 87
 - stifle joint 105, 116
- Osteosarcoma
- ischial 135

P

- Panoramic view 140
- Patella 106, 108
- Patellar luxation 105
- Pelvic girdle 122
- rectal palpation 121
- Pelvis 122
- Phalanx
- distal 26, 194, 199
 - middle 26, 32
 - proximal 16, 26, 38, 169
- Plegmon 160, 168
- distal limb 47
 - interdigital, fetlock joint 35
 - muscle 152
 - periarticular 137
 - peritarsal 103
 - tarsal 100
- Pia mater 222, 226
- Piezo-electric effect 1
- Pneumarthrosis
- arthrocentesis 25
- Polyarthritits
- septic 15
- Probe (transducer) 1
- convex 9, 12
 - crystals 1
 - curvilinear 9
 - linear 9, 11, 124
 - phased array 9
 - rectal 1, 124
- Pulsed-wave (PW) Doppler 159, 163
- Puncture
- abscess 236
 - coxofemoral joint 234, 235, 236
 - fluid collection/target area 234, 238
 - lumbo-sacral foramen 228
 - shoulder joint 234
 - tarsocrural joint 237
 - ultrasound-guided 113, 228, 233

R

- Radius 52
- Rayl 2, 3
- Reflection 2
- Refraction 5
- Regional anesthesia 211
- intravenous retrograde 159
- Region of interest 11, 139, 175
- Resolution 3
- axial 3
 - characteristics/definition 4
 - elevational 3
 - lateral 3
 - spatial 3
- Routine needle shaft 235
- Rupture
- biceps brachii muscle 148
 - collateral ligament 35, 48
 - cruciate ligament 105, 118
 - deep digital flexor tendon 142
 - digital extensor tendon 137
 - digital flexor tendon 137
 - gastrocnemius muscle 148, 153
 - ligament 142
 - long digital extensor muscle 151
 - meniscal ligament 118
 - muscle 147, 152
 - superficial digital flexor tendon 102, 142
 - suspensory ligament 142
 - tendon 142
 - third fibular muscle 105, 151

S

- Sacral tuber 122
- Sacrococcygeal epidural injection 221
- Sacrum 126
- Saphenous branch of the femoral nerve 213
- Scapula 79, 80, 81, 82, 237
- Scapular fossa 83
- Scapular region 79
- Scapular spine 81, 82, 83
- Scapulohumeral joint space 81
- Scattering (diffuse reflection) 3
- Sciatic nerve block 213, 214
- Septic inflammation
- tendon 144
 - tendon sheath 144
- Septic spavin 89, 95
- Sequestrum 175, 187
- pelvic bones 124
- Seroma 18, 22
- stifle joint 120

- Sesamoid bone 16, 138, 141
- Shoulder joint
- traumatic injuries 87
- Shoulder region 79
- Skin 13
- Sole hemorrhage 193, 202
- Sole horn
- anatomy 196
 - thickness 193, 196
- Sole soft tissue 197
- thickness 193, 200, 201
- Sonopalpation 58
- Space-occupying lesion 22
- Specular reflection 2
- Spina bifida 229
- Spinal canal 224
- Spinal cord 221, 224
- congenital malformation 222, 229
 - thickness, measured ultrasonographically 230
- Spinal ultrasound 221
- Split cord malformation 229
- Subarachnoid space 222, 223, 226
- Subchondral lesion 12
- Subluxation 18, 175, 182
- elbow joint 182
 - fetlock joint 35, 48, 182
 - radioulnar 75
- Supraglenoid tubercle 81, 82, 83
- Suspensory ligament 8, 16, 91, 92, 138, 139, 141
- branches 37, 142
 - interdigital branch 138
- Synovial cavities 11, 12
- Synovial effusion 12, 18
- Synovial herniation 22
- Syringomyelia 221, 229

T

- Tarsal region 89
- Tarsus 90
- Tear/s
- collateral ligament 35, 48
 - digital extensor tendon 137
 - digital flexor tendon 137
 - gastrocnemius muscle 148
 - ligament 142
 - meniscal 118
 - muscle 152
 - tendon 142
- Tendinitis 11
- deep digital flexor tendon 101

- Tendon/s 13
 - Achilles tendon 90, 95, 149
 - anatomy 138
 - biceps brachii tendon 81, 82
 - biceps femoris tendon 119
 - brachiocephalicus tendon 79
 - carpal radial extensor tendon 17, 18, 19, 52, 54, 137, 139, 143
 - carpal radial flexor tendon 54
 - carpal ulnar extensor tendon 54
 - carpal ulnar flexor tendon 17, 54
 - caudal tibial tendon 137
 - common digital extensor tendon 19, 26, 27, 38, 52, 54, 139
 - common digital flexor tendon 18
 - cranial tibial tendon 91, 94
 - deep digital flexor tendon 16, 17, 18, 19, 26, 28, 32, 38, 54, 90, 92, 94, 137, 139, 140, 141, 142, 144, 145, 161, 164, 194, 198, 201
 - deltoid tendon 83
 - digital flexor tendon 28, 137
 - gastrocnemius tendon 21, 91, 94, 137
 - infraspinatus tendon 79, 81, 83, 86, 87, 137
 - lateral digital extensor tendon 27, 38, 52, 54, 90, 91, 94, 139
 - lateral digital flexor tendon 92, 97, 137
 - lateral gastrocnemius tendon 102
 - long abductor tendon of the first digit 54
 - long digital extensor tendon 91, 94, 106, 107, 108, 109, 111, 118, 139, 149
 - long fibular tendon 90
 - medial deep digital flexor tendon 95
 - medial digital flexor tendon 90, 92
 - medial gastrocnemius tendon 102, 103
 - popliteal tendon 106, 108
 - psoas minor tendon 214
 - quadriceps tendon 106
 - radial carpal extensor muscle 138
 - short digital extensor tendon 92, 96
 - superficial digital flexor tendon 16, 17, 19, 21, 26, 32, 38, 54, 92, 94, 95, 102, 137, 138, 139, 140, 141, 142, 144, 145, 161, 164, 186
 - supraspinous tendon 79
 - tarsal extensor tendon 90
 - third fibular tendon 90, 106, 108, 109, 149
 - Tendon sheath/s 12
 - carpal extensor tendon 20, 51
 - carpal flexor tendon 17, 51, 164
 - carpal radial extensor tendon 51
 - caudal tibial muscle 146
 - common digital extensor tendon 27, 137
 - common digital flexor tendon 18, 137, 138, 139, 140
 - deep digital flexor tendon 26, 52, 89, 138
 - digital extensor tendon 42
 - digital flexor tendon 42
 - digital flexor tendon at the tarsus 139
 - lateral digital extensor tendon 27, 137
 - lateral digital flexor tendon 18, 37
 - long digital extensor tendon 137
 - medial digital flexor tendon 37
 - superficial digital flexor tendon 52
 - tarsal 94
 - Tenosynovitis 11, 12, 18
 - carpal extensor tendon sheath 51, 63
 - carpal flexor tendon sheath 51, 63
 - carpal radial extensor tendon sheath 18, 51
 - common digital extensor tendon sheath 51
 - common digital flexor tendon sheath 145
 - deep digital flexor tendon 101
 - digital flexor tendon sheath 35, 144
 - lateral digital extensor tendon sheath 51
 - lateral digital flexor tendon sheath 238
 - medial common digital flexor tendon sheath 144
 - tarsal extensor tendon sheaths 97
 - tarsal flexor tendon sheaths 97
 - Thin sole 193, 194, 195, 198, 201
 - Three-chamber view 139, 141
 - Thrombosis 160, 168
 - abdominal aorta 135, 172
 - arterial 168, 172
 - caudal branch of the lateral saphenous vein 8, 168, 171
 - caudal vena cava 159
 - cranial branch of the lateral saphenous vein 168, 171
 - digital vessels 47
 - dorsal common digital vein III 169
 - external jugular vein 159
 - femoral artery 172
 - fine-needle aspiration 172, 234
 - lateral plantar common digital vein 168
 - lateral plantar metatarsal vein 168, 238
 - lateral saphenous vein 171
 - limb arteries 172
 - medial plantar common digital vein 168
 - medial plantar metatarsal vein 168
 - plantar common digital vein IV 169, 170
 - tarsal veins 89, 94, 101, 159, 171
 - venous 47, 100, 103, 168
 - Tibial tuberosity 106, 108, 176
 - Total body fat (TBF) 205
 - Transducer 1
 - Tumors
 - bone-associated 192
 - pelvic region 135
 - Type-1/2 osteomyelitis 183
 - Type-1 abscess 22
 - Type-2 abscess 22
- ## U
- Ultrasonography
 - acoustic principles 1
 - continuous wave (CW) Doppler 159
 - curvilinear (convex) probes 9
 - description of findings 10
 - diffuse reflection (scattering) 3
 - documentation 10
 - examination protocol 9
 - focal zone 4
 - frequencies 9
 - linear probe 9
 - orientation 9
 - physics 1
 - preparation of the patient 9
 - probes 9
 - pulsed-wave (PW) Doppler 159, 163
 - real-time B-mode (grayscale) imaging technique 159
 - region of interest 11, 12
 - resolution 3
 - three-chamber-view 38, 41
 - transcutaneous 6, 124
 - transducer 1
 - transrectal 2, 5, 9, 124, 128, 131, 160, 163
 - Ultrasonography of
 - abscess 18, 22
 - arthritis 12
 - backfat 205, 207
 - bone-associated tumors 192
 - bones 13, 175
 - brachial plexus 217
 - bursitis 12, 19
 - cerebellar displacement 221
 - cerebrospinal fluid 228, 234
 - edema 18
 - femoral nerve 219
 - fracture 18, 132
 - hematoma 18, 22
 - hygroma 19
 - joint pouches 12
 - joints 12
 - ligaments 140
 - luxation 18, 182
 - muscles 13, 147

- nerves 211
 - osteitis 183
 - osteoarthritis 189
 - osteochondrosis 189
 - osteolysis 185
 - osteomyelitis 183
 - peroneal nerve 213
 - sciatic nerve 217
 - sequestrum 187
 - seroma 18, 22
 - sole horn 195
 - sole soft tissue 196
 - spinal cord 221, 223
 - subluxation 18, 182
 - tendons 13, 137, 140
 - tendon sheaths 12, 137
 - tenosynovitis 12, 18
 - tibial nerve 213
 - vessels 13, 159, 163
- Ultrasound-guided
- atlanto-occipital centesis 221
 - centesis 129, 234
 - collection of cerebrospinal fluid 221, 228, 234
 - epidural needle placement 221
 - fine-needle aspiration biopsy 234
 - joint interventions 233
- nerve block 211, 213, 214, 234
 - In-Plane (IP) approaches 211
 - Out-of-Plane (OOP) approaches 211
 - nerve localization 211
 - puncture 113, 228, 233
 - spinal catheter placement 221
- Ultrasound waves 1
- attenuation 3
 - emission 2
 - frequency 3
- V**
- Varicosis
- tarsal vessels 101
- Varicosity 174
- Vein/s 160
- anatomy 160
 - caudal vena cava 159, 160, 168
 - cranial femoral vein 214
 - cranial tibial vein 96, 160, 167
 - dorsal common digital vein III 38, 39, 160, 162, 167
 - dorsal metatarsal vein 161
 - dorsal pedal vein 96, 160, 166, 167
 - external jugular vein 159, 160, 168
 - lateral plantar common digital vein 168
 - lateral plantar digital vein 39
 - lateral plantar metatarsal vein 161, 165, 166, 170
 - lateral saphenous vein 8, 14, 103, 160, 166, 167
 - mammary vein 168
 - medial plantar common digital vein 39, 168
 - medial saphenous vein 160, 166, 167
 - median vein 160, 164, 167
 - metatarsal vein 90, 166
 - musculophrenic vein 160
 - normal ultrasonographic appearance 164
 - palmar common digital lateral/medial vein 160
 - plantar common digital lateral/medial vein 160
 - plantar common digital vein II 167
 - plantar common digital vein IV 162, 166, 167, 169
 - plantar lateral/medial metatarsal vein 167
 - popliteal vein 106, 109
 - radial vein 160, 164, 167
 - saphenous vein 16
- Vessels 159
- anatomy 160



Ao. Univ.-Prof. Dr. med. vet. Johann Kofler, Dip. ECBHM studied Veterinary Medicine in Vienna and Bologna, and did his doctoral thesis and habilitation at the Clinic of Orthopaedics in Large Animals of the University of Veterinary Medicine Vienna; he is working as an orthopaedic surgeon and teacher of veterinary students at the University Clinic for Ruminants in Vienna since 1986, he published about 160 articles and several book contributions.



The guide to musculoskeletal ultrasound

The ultrasound examination of the bovine musculoskeletal system is established as a routine examination in veterinary clinics worldwide. Practical veterinarians use their existing ultrasound equipment not only for gynaecological but increasingly also for orthopaedic examinations of calves and adult cattle.

This book provides specific instructions for the ultrasonographic examination of individual joints and describes particular anatomical landmarks of each region as a guide. In over 300 illustrations, international specialists present normal sonoanatomical findings and sonopathological findings of common diseases. A must have for modern cattle practitioners who want to broaden their diagnostic horizon!

LIQUID, SEMI-SOLID OR SOLID EFFUSIONS

Sonopalpation as an instrument of clinical examination

SIMPLE, NON-INVASIVE, DETAILED, AND GOAL-ORIENTED

New diagnostic possibilities for orthopaedic indications

ANATOMICAL LANDMARKS AND STANDARDIZED PROTOCOLS

With the right probe and protocol through all joint regions

VET PRACTICE Up-to-date, precise, practice-oriented!

ISBN 978-3-89993-976-7



9 783899 939767